University of Utah

Department of Chemical Engineering

[redacted]

(NASA-CR-140821) COMBUSTION CHEMISTRY OF SOLID PROPELLANTS Final Report (Utah Univ.) 71 p HC CSCL 21I

N75-11111

Unclas

G3/28 02830

DEC 1974
RECEIVED
NASA STI FACILITY
INPUT BRANCH

Salt Lake City, Utah

Distribution of this document is unlimited.

[redacted]

UNIVERSITY OF UTAH
DEPARTMENT OF CHEMICAL ENGINEERING

Final Report

on

COMBUSTION CHEMISTRY OF SOLID PROPELLANTS

September 15, 1974

This report was prepared for the National Aeronautics and Space Administration under Grant NGL-45-003-019 by A. D. Baer and N. W. Ryan

Report Approved by

A D Baer

A.D. BAER
Principal Investigator

TABLE OF CONTENTS

ABSTRACT

A description is presented of several studies of the chemistry of solid propellant combustion which employed a fast-scanning optical spectrometer. Expanded abstracts only are presented for four of the studies which have been previously reported. One study of the ignition of composite propellants yielded data which suggested early ammonium perchlorate decomposition and reaction, but limitations of both time and spatial resolution precluded establishing a quantitative conclusion. The results of a study of the spatial distribution of molecular species in flames from uncatalyzed and copper or lead catalyzed double-based propellants support previously published conclusions concerning the site of action of these metal catalysts. A study of the ammonium-perchlorate-polymeric-fuel-binder reaction in thin films, made by use of infrared absorption spectrometry, yielded a characterization of a rapid condensed-phase reaction which is likely important during the ignition transient and the burning process.

I. INTRODUCTION

This report is presented as a summary of research done under NASA Grant NGL-45-003-019 over the total period of the grant from October 15, 1965 to July 1, 1974. The results of many of the projects discussed here have been published in theses, reports and journal articles. In the case of such projects, only an expanded abstract of the work is presented here; the interested reader is referred to the prior publications. The last two sections of the report describe work that has not been published in generally available sources, and the description of these projects is presented here in some detail. Each section of the report contains the cited figures, tables, nomenclature, and each presents the principal conclusions derived from that project. All references cited, however, are collected at the end of the report.

The principal theme of all projects was the chemistry of solid propellant combustion, and various aspects of this broad subject area were studied experimentally and analytically. A primary tool of all the experimental work was a fast-scanning optical spectrometer. This unit was purchased from the Control Instrument Division of the Warner and Swasey Company by use of both grant and University funds. The particular Model 501 Rapid Scanning Spectrometer could be operated to yield, as electrical signals with wavelength linearly related to time, simultaneous spectra in dual wavelength (μm) ranges of 0.30 - .44 and .43 - .65; .65 - 1.15 and 1.10 - 1.79 and, 1.7 - 3.2 and 3.2 - 4.7 μm and scan repetition rates of 8, 80, and 800 per second. Single ranges of 2.5 - 5.5 μm and 5.5 - 9.0 μm were also used. Figure 1 shows the spectrometer system and illustrates how the unit was employed in these studies. In each case, a special burner or other type

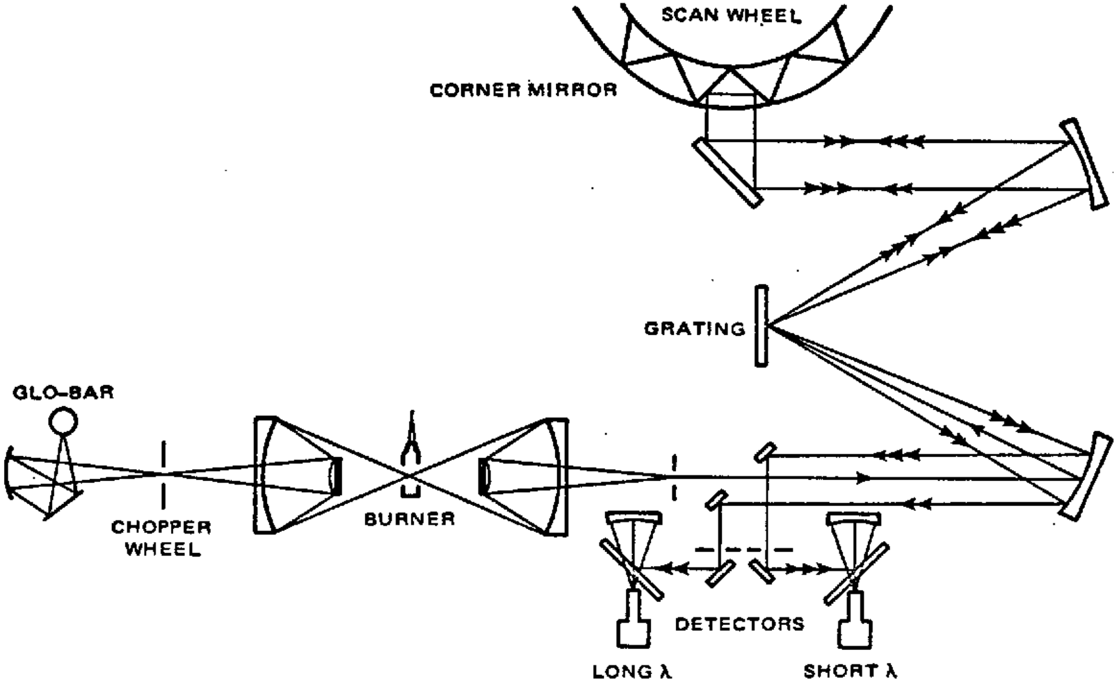

FIGURE 1. A schematic of the rapid-scanning spectrometer. The silicon carbide Glo-Bar was the source of infrared radiation in the early studies. The chopper wheel was used when alternate measurements of emission and emission-absorption spectra were required. The various test burners were placed at the common focus of the two Cassegrainian optical systems.

of apparatus was designed and built for the particular study. The observable optical phenomenon of interest was positioned at the common focus of the spectrometer and a radiation source unit. Transient tests were conducted and the spectrometer output was recorded by photographing the spectrometer output as displayed on an oscilloscope screen. The oscilloscope was normally operated without a horizontal sweep and a strip camera was used to generate the time (or wavelength) scale.

The spectrometer system was supplied with a silicon-carbide infrared source unit which was used during the earlier studies. This system was modified in our laboratory to use a vitreous-carbon element as the source of high intensity infrared radiation. The modified infrared source unit was used for the study described in Section VII.

II. AMMONIUM-PERCHLORATE DIFFUSION FLAMES

Diffusion flames between a body of ammonium perchlorate (AP) and various fuel sources—solid polybutadiene-acrylic-acid copolymer or gaseous methane or hydrogen—were investigated spectroscopically over a wavelength range of 0.3 to 5.5μ with the millisecond scanning spectrometer. Figure 2 shows the diffusion flame burner used.

A brief study was made, which did not employ the spectrometer, in an effort to further evaluate the performance of this device as a large scale model of the AP-PBAA diffusion flame. Regression rates at atmospheric pressure of the ammonium perchlorate discs were measured to be about 0.02 cm/sec for AP and binder temperatures of 275-290°C at the time of ignition. Under these conditions, the mass combustion ratio of PBAA/AP was always very nearly 0.2 or equivalent to a nearly 84 percent AP propellant which is near

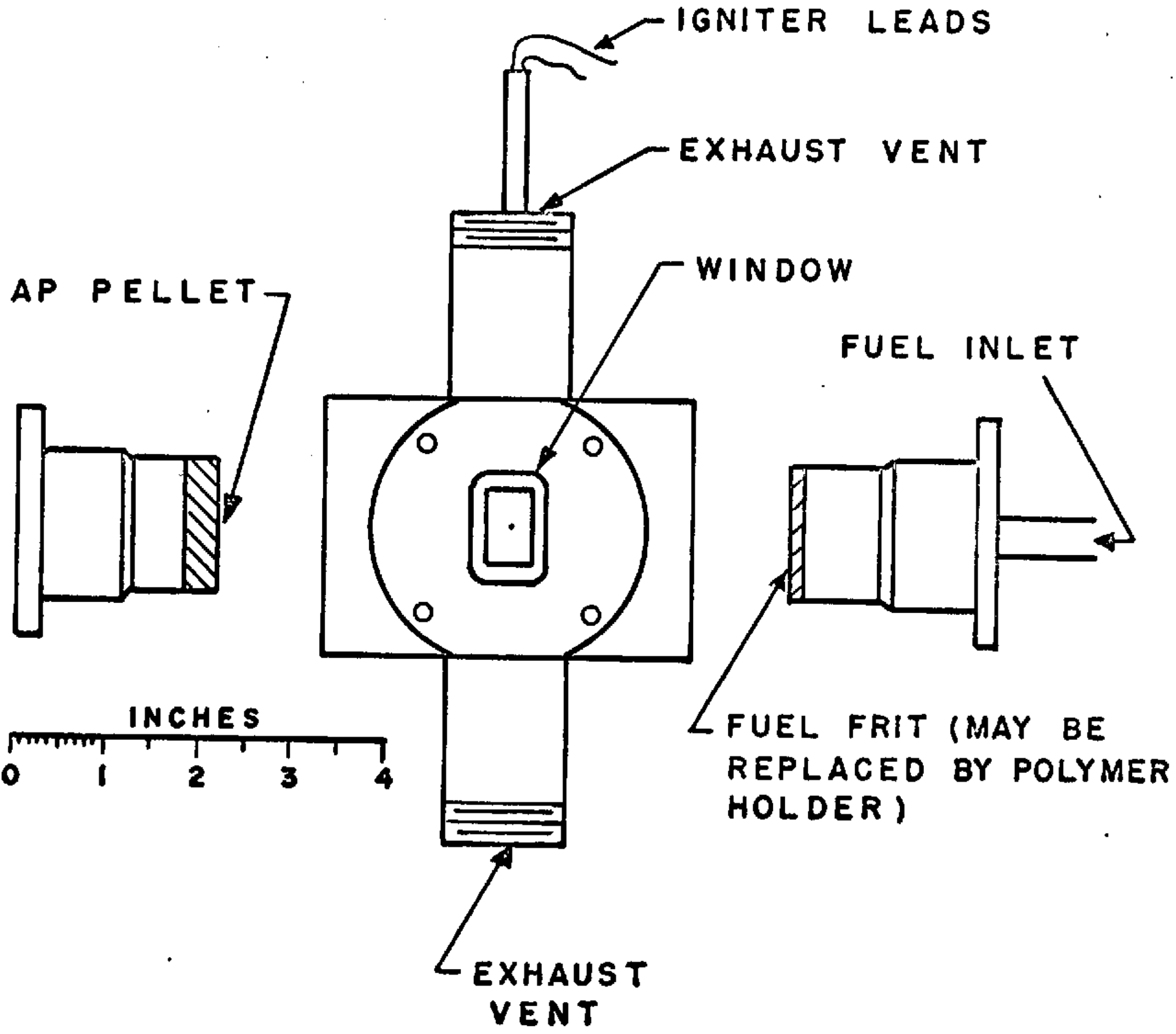

FIGURE 2. An exploded sketch of the AP-fuel diffusion flame burner. The AP pellet holder and the fuel source were mounted in the central block to center the flame in the window.

to the ratio for maximum adiabatic flame temperature. If the AP and binder temperatures were raised above 300°C, spontaneous ignition of the AP occurred and the AP was consumed with little combustion of the fuel-binder.

With gaseous fuels, the flame was approximately in the center of the gap between the fuel source and the surface of the AP. An AP-*vs.* AP flame was produced, but it was totally nonvisible to the eye. The polymer flames were very close to the fuel surface. Spectograms are published for the hydrogen-*vs.*-AP, methane-*vs.*-AP, AP-*vs.*-AP, and polymer-*vs.*-AP flames in the 1.9 to 4.7μ range [1, 2, 3].

For the methane-*vs.*-AP flame, temperatures of about 2400°K were measured by a sodium-D-line-height-comparison technique as a subsidiary study. No significant variation in the temperature across the gap was revealed by this technique.

Molecular species CO_2, H_2O, HCl, CH_4, and probably N_2O were detected in the flames. Carbon monoxide could not be detected. HCl emission was observed as near the surface of the polymer as it was possible to observe; however, it was not detected near the AP surface. Similar results were obtained in the gaseous-fuel flames. It is concluded that HCl was not a primary product of the gasification of AP.

Carbon dioxide emission was observed as near the surfaces of the fuel sources as could be observed, note Figure 3. Reactive oxidizer species must survive the flame and diffuse to this location to react with the fuel. The CO_2- and HCl-emission distributions across the gap are explained by postulating that a chlorine-oxygen compound, perhaps ClO or ClO_2, was a product of the gasification of AP and that a portion of it diffused to the fuel surface, where it oxidized the gasified fuel. In the polymer-*vs.*-AP flame, this compound may have participated in the degradation of the fuel.

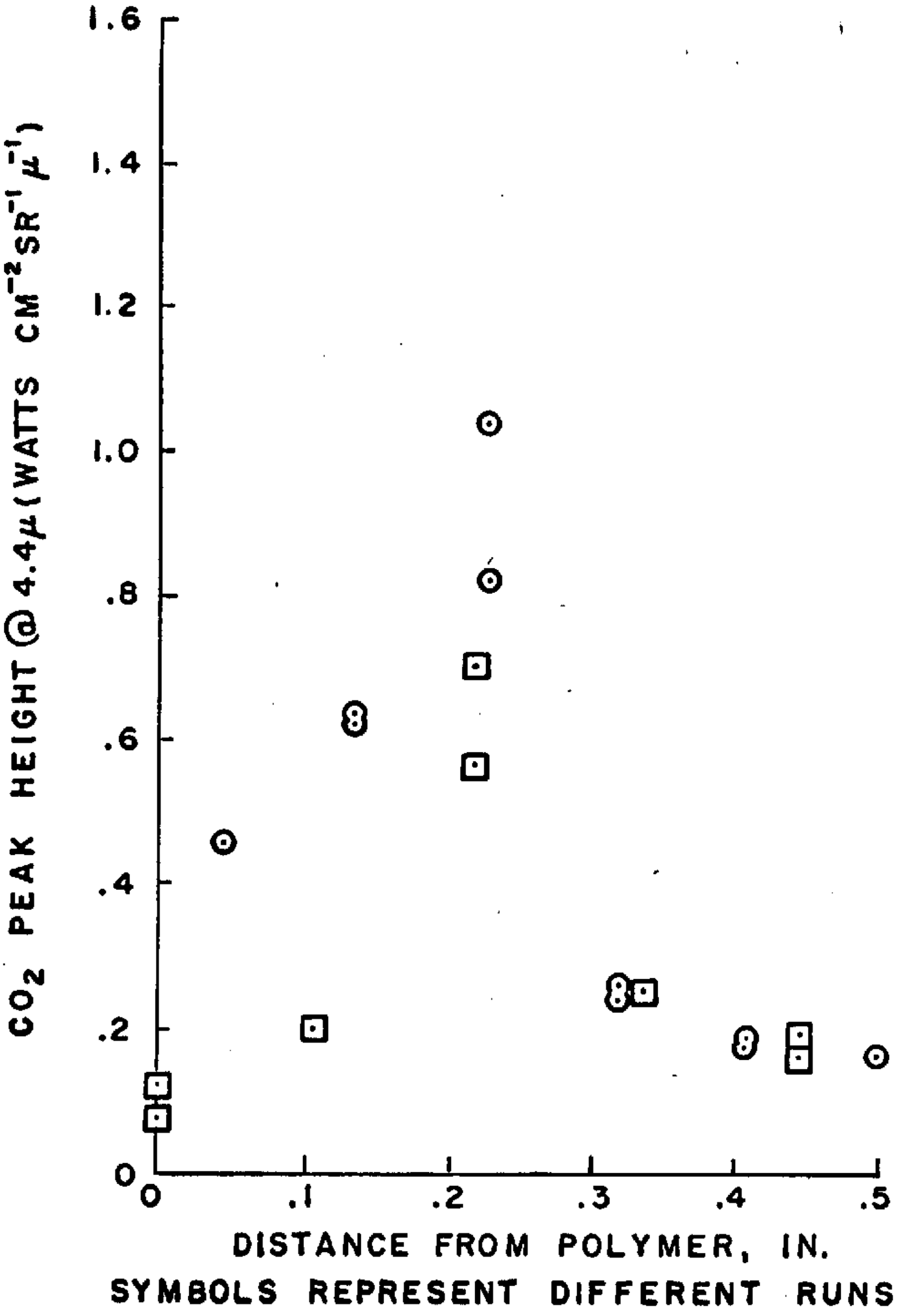

FIGURE 3. Measured intensities of the 4.3-μm CO$_2$ band for a test with ammonium perchlorate and the PBAA fuel binder.

III. SPECTRA NEAR THE SURFACE OF AN IGNITING PROPELLANT

Figure 4 shows the imaging furnace, featuring an L-shaped optical pathway between two 21-inch, first-surface elliptical reflectors, which was designed and built for use in conjunction with the rapid-scanning spectrometer. This imaging furnace featured rapid shuttering by rotating a plane folding mirror positioned at the coincident secondary foci of the two reflectors. The rapid-scanning spectometer was used to characterize the pre-ignition, ignition, and early flame development phases of solid propellant combustion [4].

Data were obtained at the 1-msec scan time of the spectrometer for the 0.3- to 0.65-micron and 1.7- to 4.8-micron ranges of the instrument. Catalyzed and uncatalyzed PBAA-AP propellants were studied. The uncatalyzed propellant contained 4.1 weight percent $NaClO_4$ so that D-line emission could be used as a criterion of ignition. Ignition times from 0.2 to 1.0 seconds were observed at atmospheric pressure. The spectrometer focus was positioned 0.2 to 0.3 cm in front of the 1-cm diameter sample surface.

The only species present at detectable concentrations in the near infrared range were CO_2 and H_2O. Possible gaseous pre-ignition species such as $HClO_4$ or ClO_3 were not seen, but the instrument sensitivity may not be great enough to permit observing them.

The presence of the CO_2 spectra, shortly following ignition by radiant heating from the imaging furnace, suggests that the AP is the first constituent to decompose since it is the significant source of oxygen. CO_2 formation preceeds that of H_2O indicating that the ammonium perchlorate partially decomposes first, its products attacking the polymer and/or the polymer decomposition products. Little more can be said from the results here

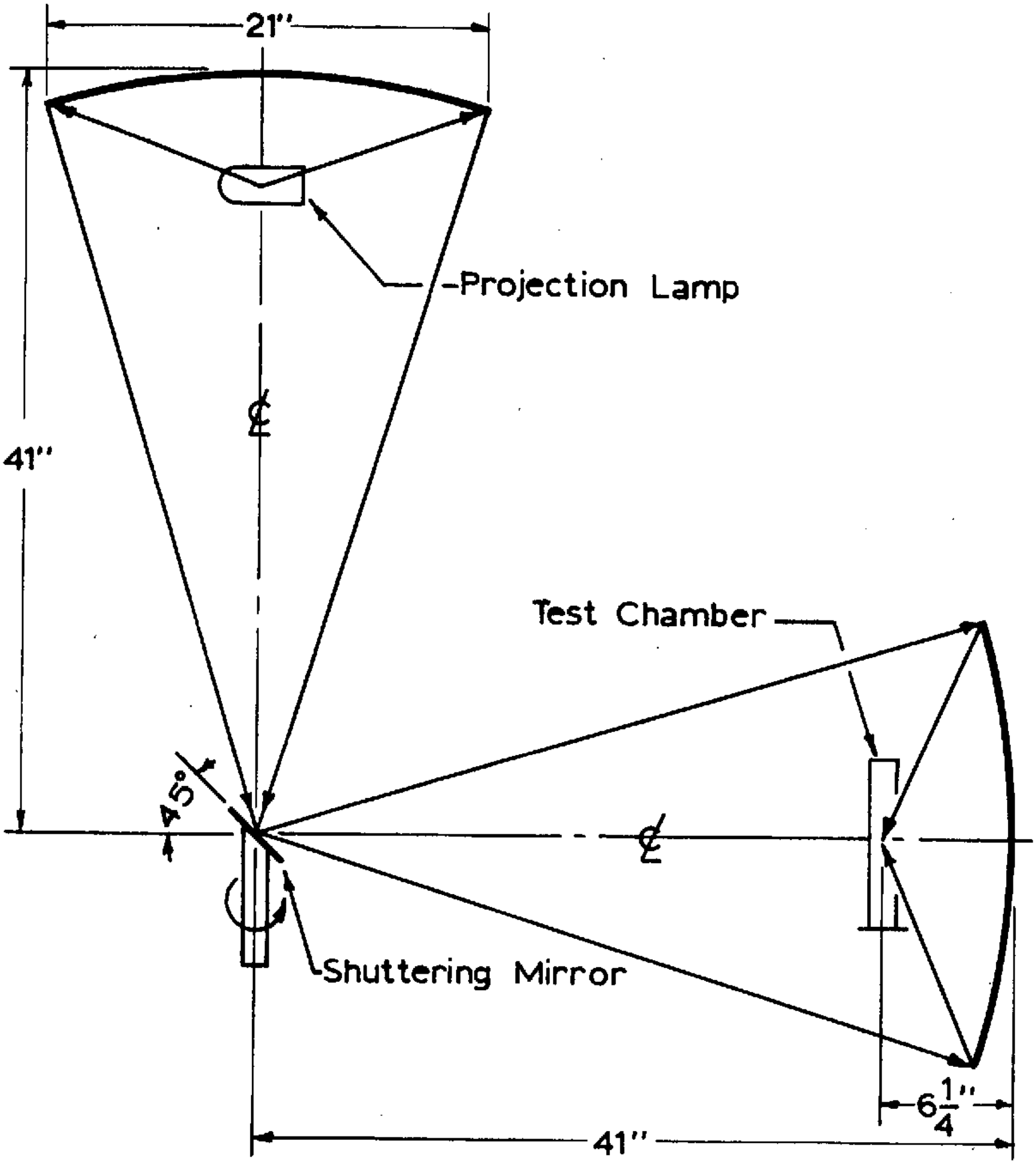

FIGURE 4. A schematic diagram of the imaging furnace. Note that the optical pathway from the collecting reflector to the re-imaging reflector is folded at the secondary focii of these reflectors to give an L-shaped optical pathway.

concerning the CO_2-H_2O reaction products, but the suggestion is made that by quantitatively monitoring these two species some understanding may be obtained concerning the AP-PBAA reactions.

The sodium D-line emission was the only detectable line emission in the 0.3-0.65 micron range. Not even metallic line emission from the copper chromite-catalyzed propellant was observed from the 1-cm diamater, atmospheric flame. An interesting phenomenon was observed associated with the burning of a semi-transparent AP-PBAA propellant. When an incident radiation of 10-20 cal/(sec)(cm^2) was directed at the surface of this propellant, the visible spectra indicated periodic great increases in the sodium line intensity followed by a 1- to 2-msec period of greatly increased continuum in both the 0.3-0.41 and 0.4-0.65 spectral ranges. Figure 5 shows this sequence.

This phenomenon ceased when the incident radiation ceased. Apparently the external radiation caused heating in depth, and perhaps, sub-surface explosions which both increased the concentration and temperature of the sodium and particulate material in the optical path of the spectrometer. Also, the use of the sodium D-line may prove to be a very accurate, refined method for determining the point of ignition if it can be shown that this event is coincident with the occurrence of the sodium D-line.

IV. SPECTRA AND TEMPERATURE OF PROPELLANT FLAMES DURING DEPRESSURIZATION

The millisecond-scan-time spectrometer was used to obtain emission spectra from composite-rocket-propellant flames in the wavelength range of 0.3 to 4.8 microns at pressures from 0.5 to 6.0 atmospheres during steady burning and during rapid depressurization in a rarefaction tube. Figure 6 shows the experimental system. Ammonium-perchlorate-oxidized composites

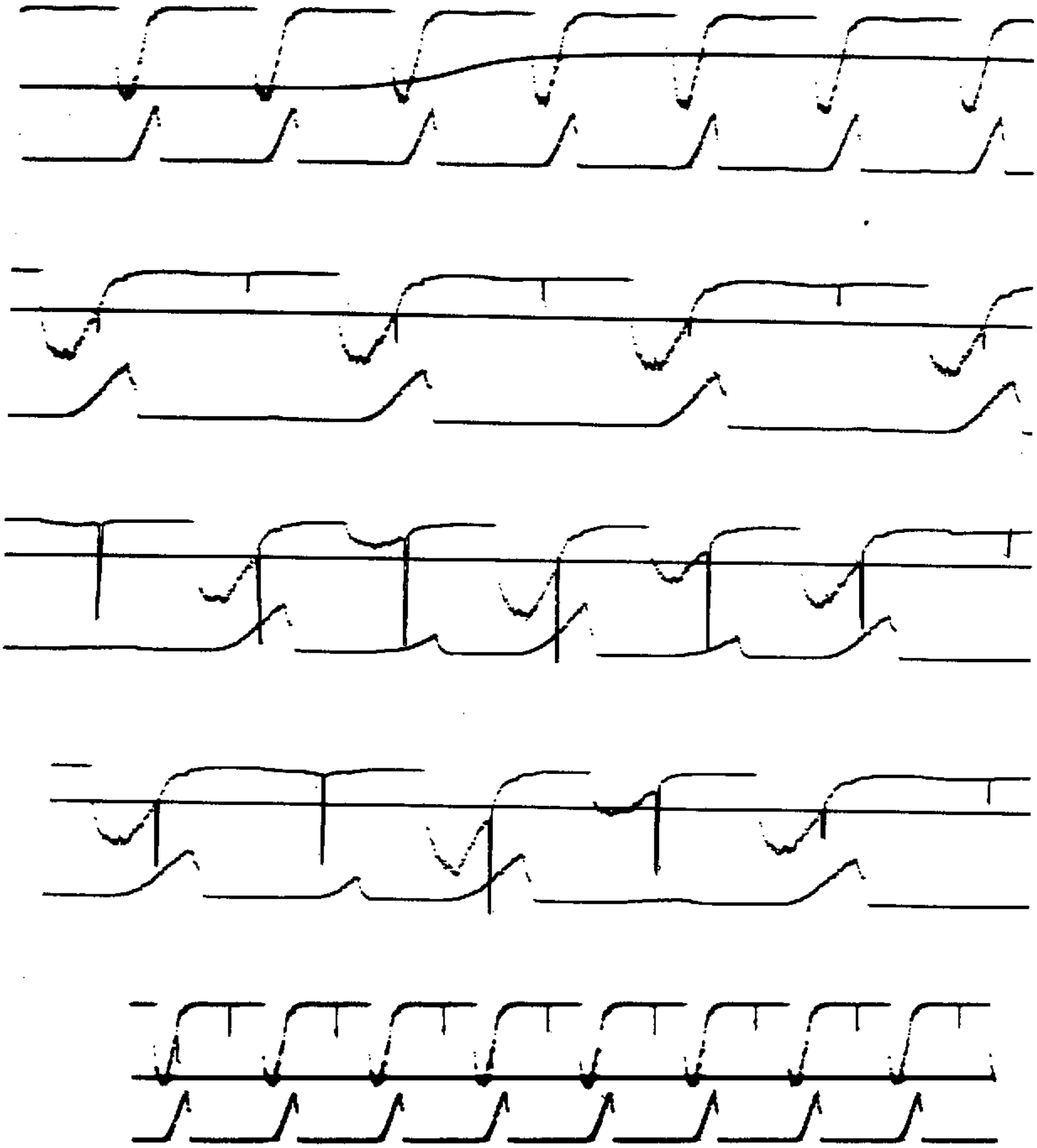

FIGURE 5. A series of sequences taken in the visible spectral region. The spaces between the traces indicate the camera speed since the scan rate is constant at 800/sec. The top sequence shows the shutter opening, time and wavelength increasing to the right. The upper trace is the long wavelength signal. The center trace is a photocell output which measured the reflected light from the sample surface. The second sequence shows the early appearance of the sodium D-line. The third and fourth sequences show unexplained spectral "eruptions." The fifth sequence shows the spectral patterns after the imaging furnace had been cut off.

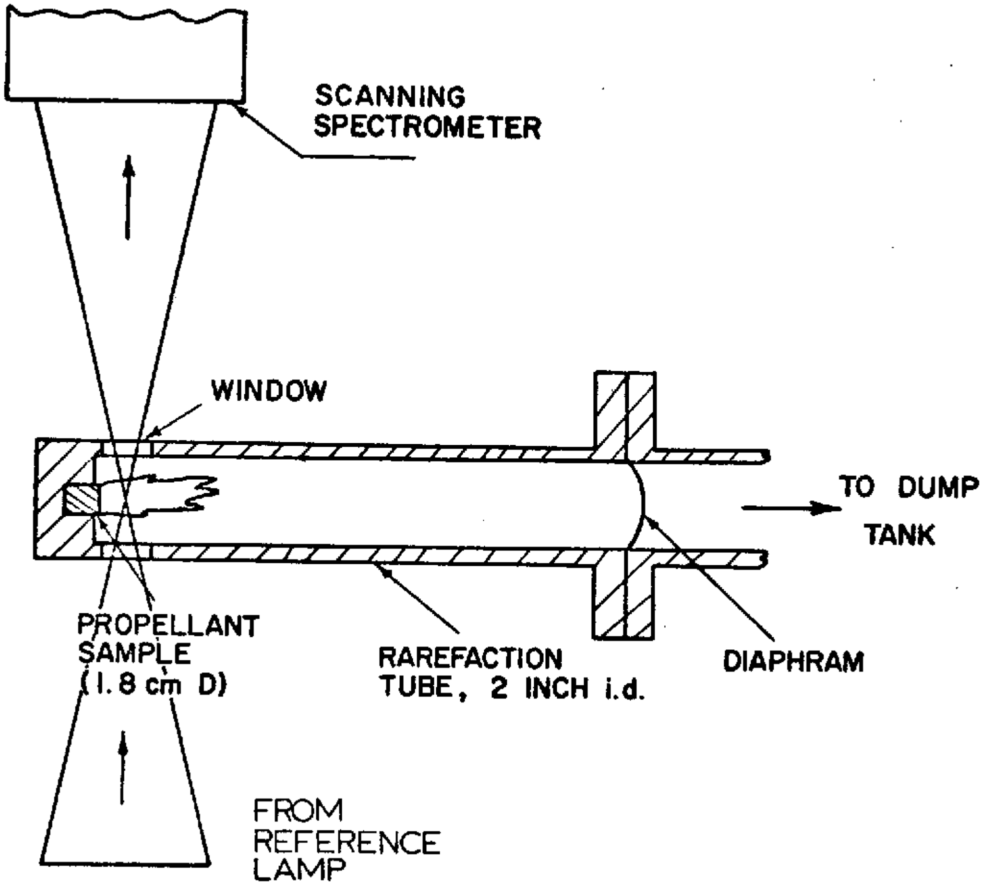

FIGURE 6. The system used to obtain flame spectra during depressurization extinguishment is illustrated here.

which contained conventional fuel binders (PBAA, polyurethane, polyfluorocarbon) were studied. Details of this work are presented in references [5, 6, and 7].

The changes in the emission spectra during steady combustion produced by variation of the ammonium-perchlorate-to-binder ratio in the propellants were determined. The ammonium-perchlorate content (78 to 86.5 percent) of the propellant was found to have a strong effect on the ratios of emission intensity at 2.5, 2.9, and 3.15 microns, which resulted principally from water, to the emission intensity of carbon dioxide at 4.3 microns. These water-to-carbon-dioxide emission-intensity ratios decreased as the oxidizer loading was increased. This apparent decrease in the water-to-carbon-dioxide concentration ratio with increase in oxidizer loading is in qualitative agreement with the computed decrease in this concentration ratio for equilibrium flames.

Burning propellant samples were subjected to pressure changes produced by the two-inch-diameter rarefaction tube, which generated essentially constant fractional pressure-decay rates. For the fractional depressurization rates employed ($d \ell n P/dt = -5$ to $-20 \sec^{-1}$), the most important extinguishment parameter was the exhaust pressure of the rarefaction tube, although this minimum pressure was always much greater than the propellant low-pressure deflagration limit. As seen in Figure 7, the transient emission spectra showed a decrease in the water-to-carbon-dioxide intensity ratios during rapid pressure drop, which based on steady-state measurements indicated that the ratio of oxidizer to binder species in the gas phase initially increased. The relative rates of decomposition of the propellant constituents was apparently changed, with the oxidizer rate being higher during the pressure decay.

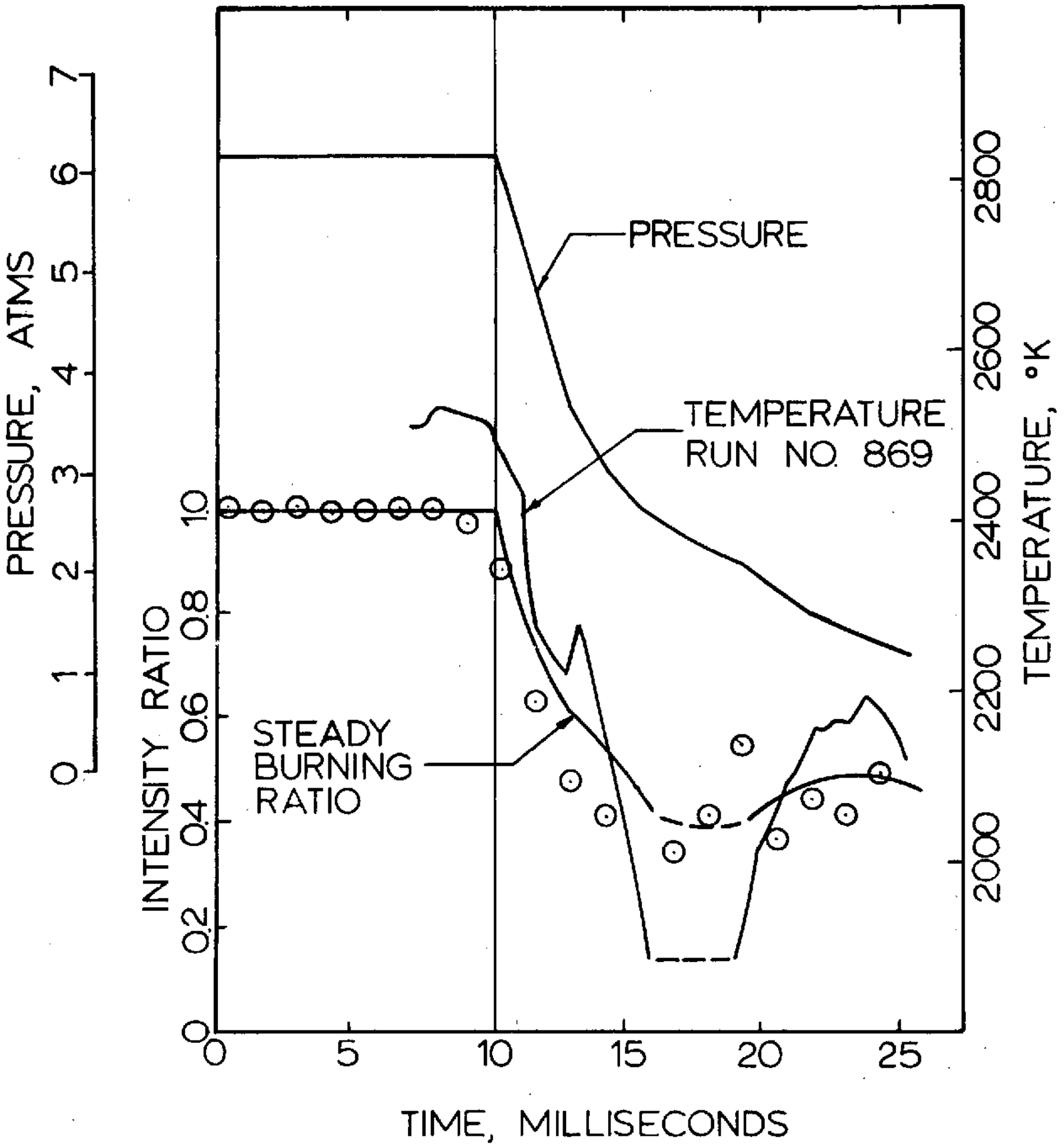

FIGURE 7. Flame-temperature and emission-intensity ratios from separate but nearly identical tests. This test was with an 82% AP-PBAA composite. The normalized "intensity ratios" is for the ratio of emission at 2.5 μm from water to 4.3 μm from carbon dioxide. The steady-burning ratio was computed from steady-state data at the same pressure and is corrected for the shift in the black-body radiation-intensity ratio as temperature is changed.

Later, as the rate of pressure drop decreased, the ratio of oxidizer to fuel in the flame decreased as a result of the apparent depletion of the surface ammonium perchlorate. Recent results [9] obtained by use of absorption spectrometry suggest that this interpretation of the emission spectra data may not be valid, and that the polymer may actually increase its pyrolysis rate relative to the ammonium perchlorate during pressure decay.

Tests were also made by subjecting burning samples to alternating periods of falling and then rising pressure. The water-to-carbon dioxide emission-intensity ratio, which originally dropped, was observed to rise above the initial value during the pressure rise. The emission-spectra data are interpreted as resulting from nearly independent fuel and oxidizer decomposition during pressure change.

An attempt was made to obtain direct evidence of this independent-decomposition postulate by use of propellants formulated with ammonium perchlorate containing various spectrally identifiable co-precipitated compounds and with fuel binders containing other identifiable materials. The results of these tests were inconclusive. Figure 8 shows typical data. It was found that an effect of the additives was to produce changes in the response of the infrared flame spectra to pressure variations, which indicated that the apparent oxidizer-to-fuel ratio in the flame always remained nearly constant. For the additive-containing formulations, an interaction in the decomposition process of the oxidizer and fuel is suggested by this result. Propellant formulations which indicated a large shift in the fuel-to-oxidizer ratio during depressurization were found to be easier to extinguish than propellants which contained metallic additives and which did not indicate such response. Thus, if independent decomposition of the binder and oxidizer during depressurization promotes extinguishment, the solid propellant

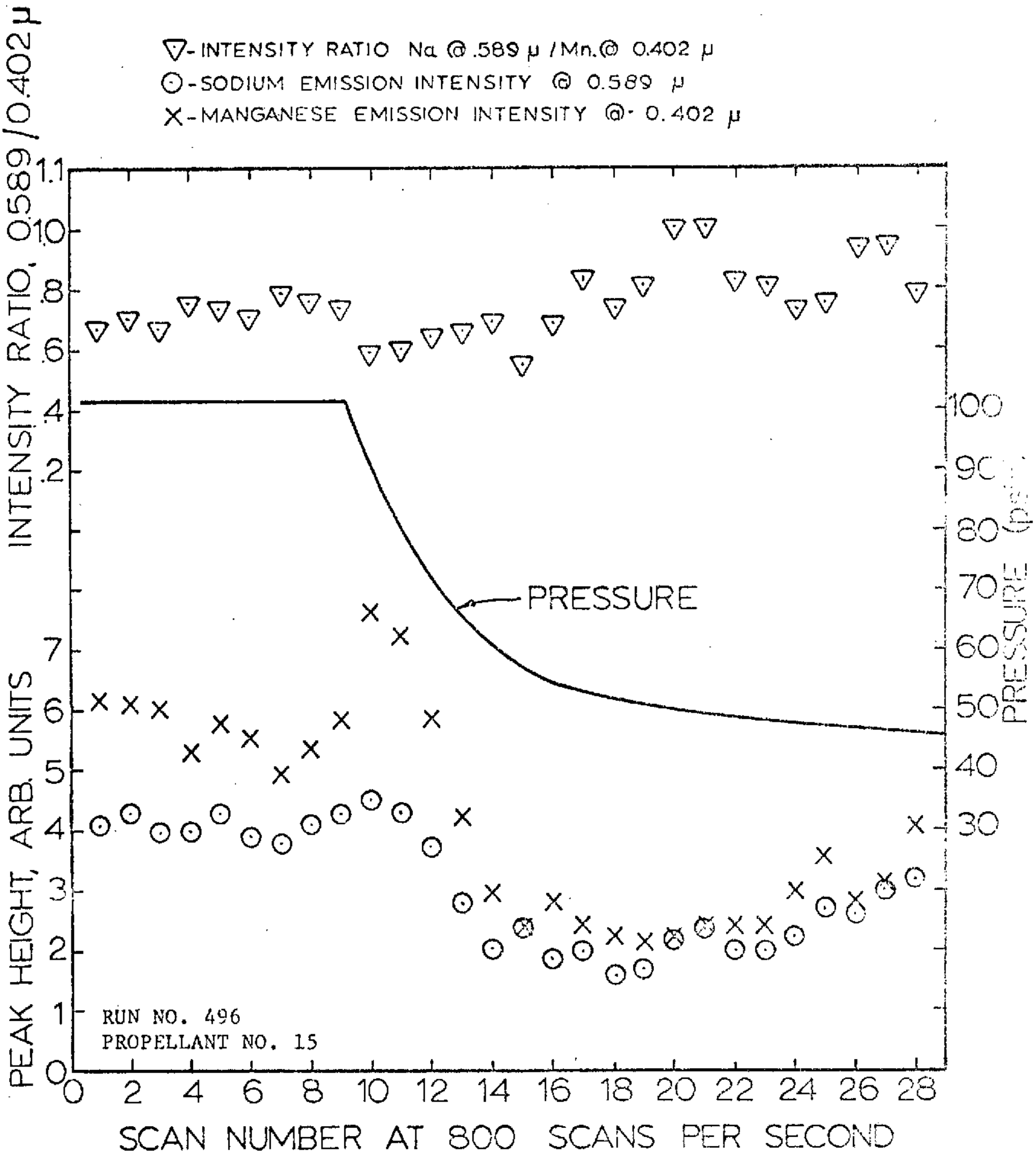

FIGURE 8. Relative sodium and manganese emission intensities and the Na/Mn ratio during depressurization are plotted here.

that is to be used in a stop-restart application should be of simple composition.

Propellant-flame temperatures were determined by an absorption-emission measurement at the wavelength of the sodium D-lines. The agreement between calculated adiabatic flame temperatures and measured steady-state temperatures was within the anticipated experimental error (20 to 50°K at 2200 to 2900°K) for all sodium concentrations and spectrometer settings employed. Figure 7 shows that during depressurization the flame temperatures changed rapidly. These temperature measurements show that the assumption of a nearly constant flame temperature during depressurization is invalid and that the theories which predict a monotonically decreasing gas temperature during pressure decay are not general.

V. SPECTRA OF PROPELLANT FLAMES DURING UNSTABLE COMBUSTION

A program was undertaken to observe spectral details of the flames of composite solid propellants during unstable combustion in an attempt to further elucidate the processes involved. This program was motivated by the inconsistencies between experimental observations of burning solid propellants and theoretical modeling of the same, particularly in the area of unstable combustion. References [10] through [12] discuss this work in detail.

In order to accomplish this end, the rapid-scanning optical spectrometer was employed at a scan rate of 800 scans per second. This instrument was operated in the middle infrared region of the spectrum from 1.7 μm to 4.8 μm. Figure 9 shows the special low L* burner which was designed to achieve a continuously variable volume and which was provided with purged

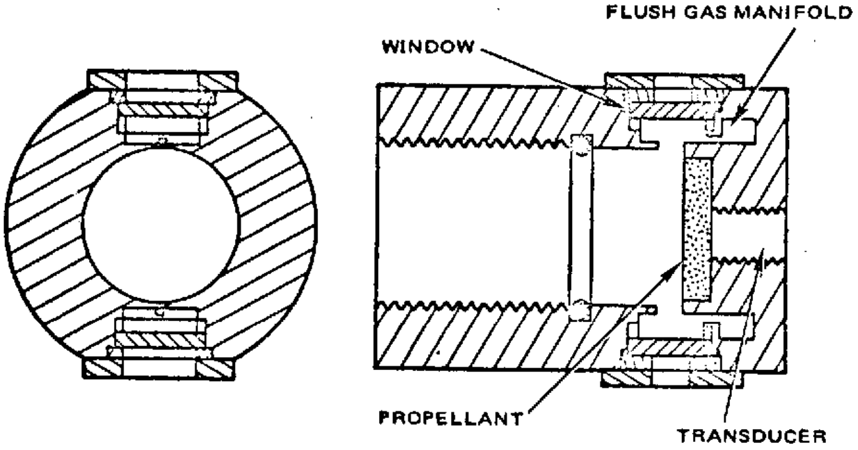

FIGURE 9. The continuously variable volume L* burner with purged view ports is sketched here.

sapphire windows that allowed observation of radiation of wavelengths to 5 μm. A series of ammonium perchlorate-polyurethane propellants were formulated which, although identical in composition and indistinguishable from each other in net burning rate, produced low L* instability at frequencies from 10 to 100 Hz at pressures from 20 to 60 psia as a function of ammonium perchperchlorate particle size.

Use of this system allowed measurements of temperature and composition relative to chamber pressure. From these measurements,phase and time differences were determined. At least three different varieties of unstable combustion were observed; sometimes simultaneously. These are described as bulk mode instability, "layer frequency" instability, and local intrinsic instability.

Preliminary to combustion tests in the L* burner, burning rate determinations were made indicating that the average burning rate *versus* pressure relationships for the series of propellants used were indistinguishable within the experimental uncertainty. However, where observed photographically and determined as a function of time it was clear that on the time scale of the oscillatory phenomena observed, no unique burning rate could be assigned to the propellants. An oscillation in the irregular burning rate very nearly at the frequency predicted by the "layer frequency" theory for the coarse ammonium perchlorate was apparent. This frequency could subsequently be seen superimposed on the higher frequency oscillations of the low L* tests.

Spectroscopic measurements of composition and temperature were made during stable and unstable combustion tests using a 1.25 millisecond scan repetition rate over the 1.7 μm to 4.8 μm region of the infrared spectrum. These measurements indicated that there were fluctuations in composition and temperature which were coupled to the pressure oscillations in a manner not incompatible with that predicted by grossly simplified theories of L* instability in terms of lead time of the combustion oscillations relative to those of the pressure. Figure 10 shows an example of this type of behavior. In addition there were composition fluctuations seen which were not coupled to the pressure fluctuations, but which apparently were associated with the coincident temperature fluctuations. These were local oscillations due either to local fuel to oxidizer ratio fluctuations or to burning rate fluctuations. These local fluctuations in flame character were even seen during otherwise stable tests at constant chamber pressure. Figure 11 shows an example of the coupling of these "intrinsic" instabilities and the bulk mode phenomena.

Several general observations may be made. First, there is no such thing as a one-dimensional surface or flame zone in the combustion of many solid propellants. And, further, in the case of composite (or composite modified double base) propellants, homogeneity is also a fiction. On the other hand, it appears that at these low frequencies (10 to 100 Hz) the quasi-steady gas phase approximation is valid in that instantaneous equilibrium seems to be maintained.

VI. EFFECTS OF CATALYSTS ON THE INFRARED FLAME SPECTRA OF DOUBLE-BASE PROPELLANTS

The fast-scanning spectrometer was also employed in a study of catalyst effects in double-based propellants. Although the principal support for this research was not supplied by the NASA grant funds, this work is reported here since it was related to the general area of chemistry of solid propellant combustion. Dr. V. M. Mal'tsev of the Institute of Chemical Physics, Moscow,

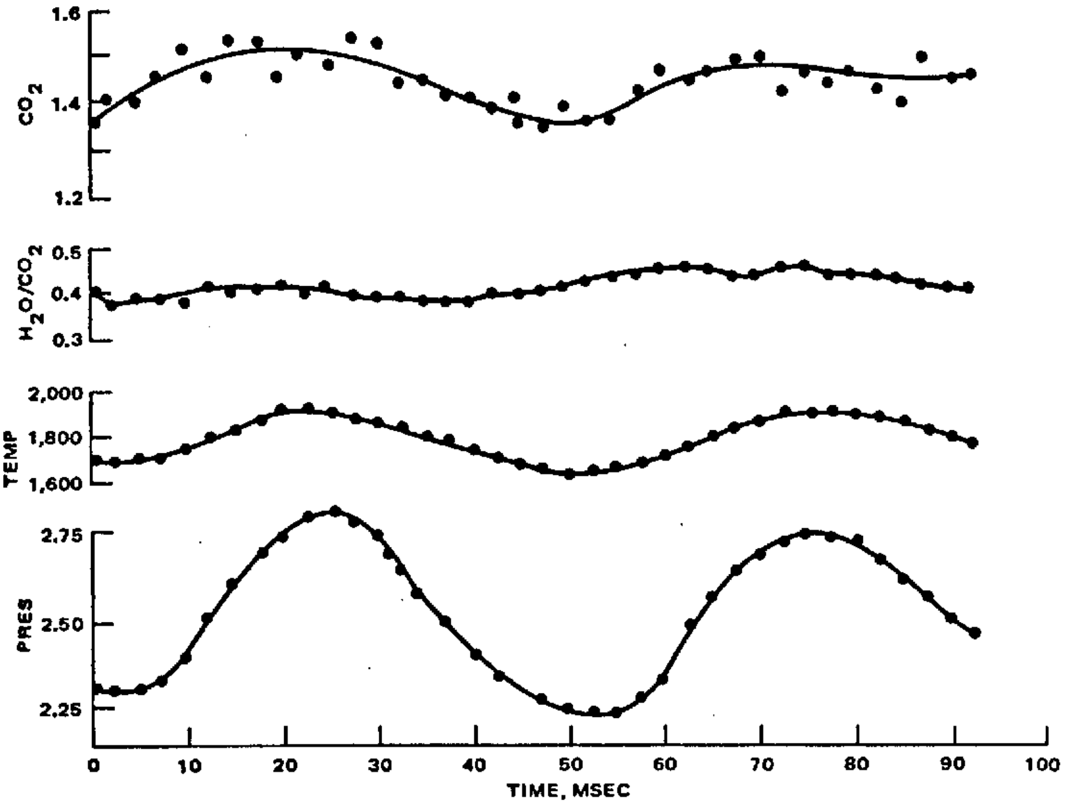

FIGURE 10. An example of bulk instability

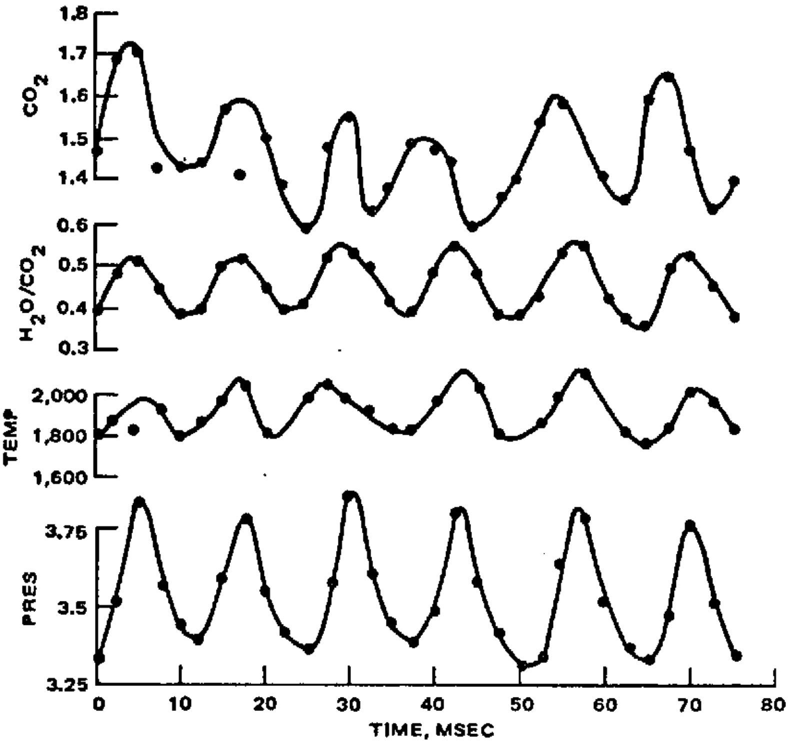

FIGURE 11. An example of coupled bulk mode and intrinsic instabilities

USSR was a visitor in our laboratory from November 1971 to March 1972 under the auspices of the U. S. Academy of Sciences. While here, Dr. Mal'tsev conducted a short research program to obtain infrared spectra data from various double-base propellant flames to supplement his prior results obtained in the USSR and at Princeton University. This work was intended to determine the site of the catalytic activity of copper and lead in the double-base propellant systems.

The work by Mal'tsev and Summerfield [12] on the effect of platonizing catalysts on the visible and ultraviolet spectra of nitrate-ester propellants suggested that lead compounds may accelerate decomposition in the near-surface region of the condensed phase, while copper compounds appear to act in the near-surface region of the gas phase. Because of the long, 1-2 cm, reaction zone of the double-base propellant flame at pressures below 15 atms , it is possible to make spatially resolved measurements of this reaction zone with the fast-scanning spectrometer, and this study by Dr. Mal'tsev was conducted employing this spectrometer in the infrared region to evaluate the conclusion from his previous study [13].

The conclusion cited is based partly on visible and UV emission spectra which signify excited species that may not be important participants in the reactions. The present study was motivated by a desire to check the conclusion, and perhaps gain some knowledge about the gas-phase kinetics. The method is to observe spectra in the infrared, where the important species are manifested in their near equilibrium energy states.

A special 2-inch diameter, high-pressure burner was placed at the common focus of the spectrometer source unit and the receiver. The original 7-inch length of the burner was extended to fifteen inches to reduce recirculation observed with the shorter length. Helium pressurizing gas was introduced behind a drilled distribution plate, to further reduce recirculation and to eliminate bouyancy effects which affected the horizontal flame. The pressure was measured from a tap located in the side of the burner with a Bourdon gage. All of the tests were taken at the 100-millisecond scan rate of the spectrometer. The output from the detectors was amplified and recorded off an oscilloscope with a 35-mm Beatie-Coleman camera operated as a strip camera. Data were obtained by use of all ranges of the spectrometer which permitted evaluation from 0.6 to 9.0 μm.

The 2.5-cm long by 0.63-cm square propellant samples were ignited by use of an electrically-heated carbon thread. The sample length was such that the ignition transient was eliminated prior to the time the surface burned past the spectrometer focus. From a knowledge of the strand burning rate and the scan time (122.3 milliseconds) in principal, the distance between the focus and the surface could be determined. But, due to the lack of radiant transmission close to the surface, due to dispersion by particles, it was necessary to estimate the surface plane to be 1.5 to 2.0 mm from the position where first indication from the spectrometer source unit was detected.

Species identified with some confidence are CO_2, CO, H_2O, N_2O, and aliphatic -CH. NO_2 was not seen. A strongly-emitting species whose emission appears through the whole length of the flame, indicating high stability of flame temperatures, appears at 4.85 μm. It does not appear in the flame of a composite propellant which contains nitrogen only as ammonium; it is therefore tentatively associated with the nitrogen-oxygen bond, possible as $R\text{-}O\text{-}NO_2$.

Emission intensities, normalized by emission intensity of the spectrometer Glo-Bar source at the same wavelength (but lower temperature), are plotted on Figures 12, 13, and 14 as functions of distance from the burning

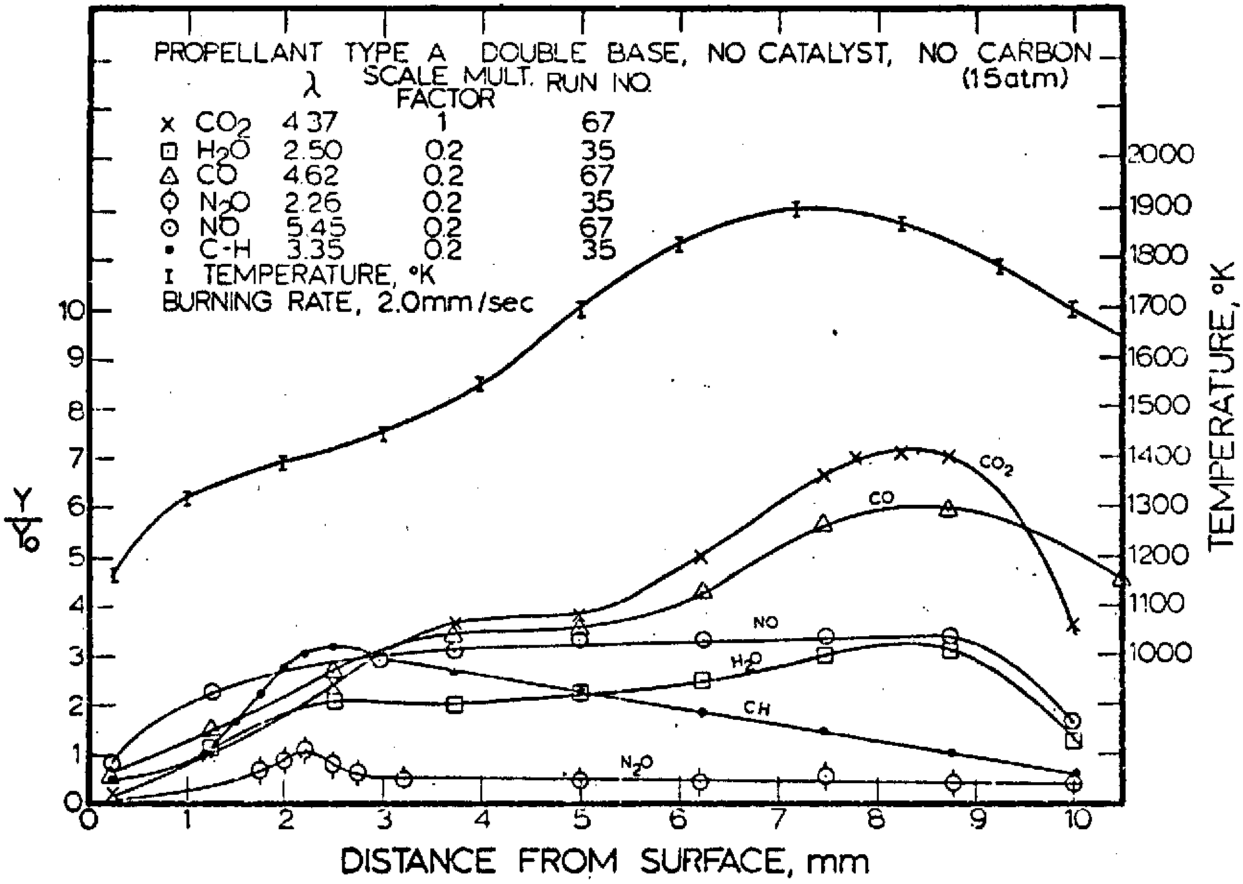

FIGURE 12. Radiation intensities from molecular species in a propellant flame are shown as a function of the distance from the burning surface. Intensity at a wavelength, Y is referred to the intensity, Y_0, of the spectrometer source unit at the same wavelength. This propellant contained 53.7 percent metriol trinitrate, and 7.0 percent tethylene glycol trinitrate.

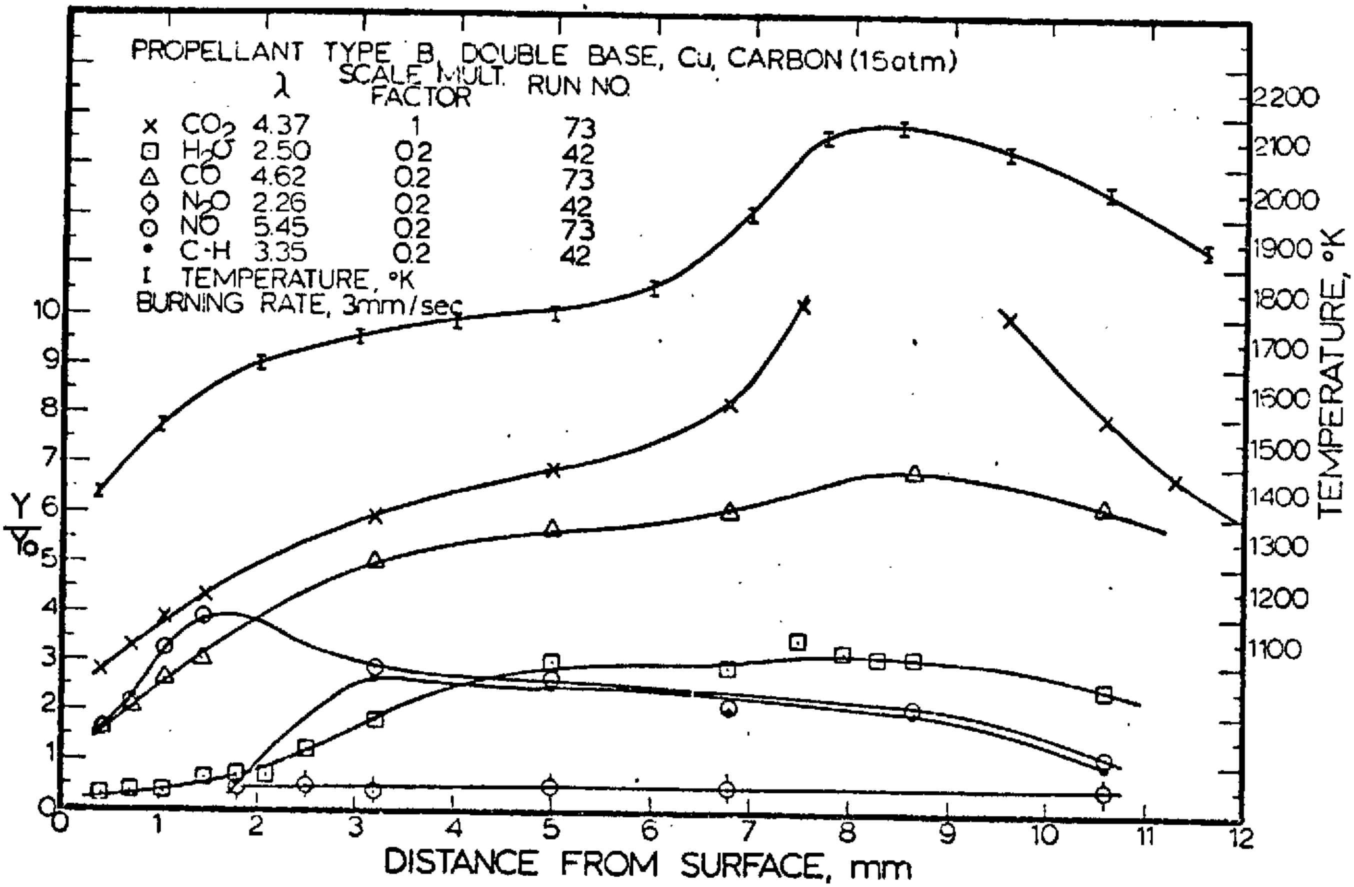

FIGURE 13. Radiation intensities from molecular species in a propellant flame are shown as a function of distance from the burning surface. This propellant is the same formulation as propellant type A (Figure 12) except it contains 0.1 percent carbon black and 1.0 percent copper salicylate.

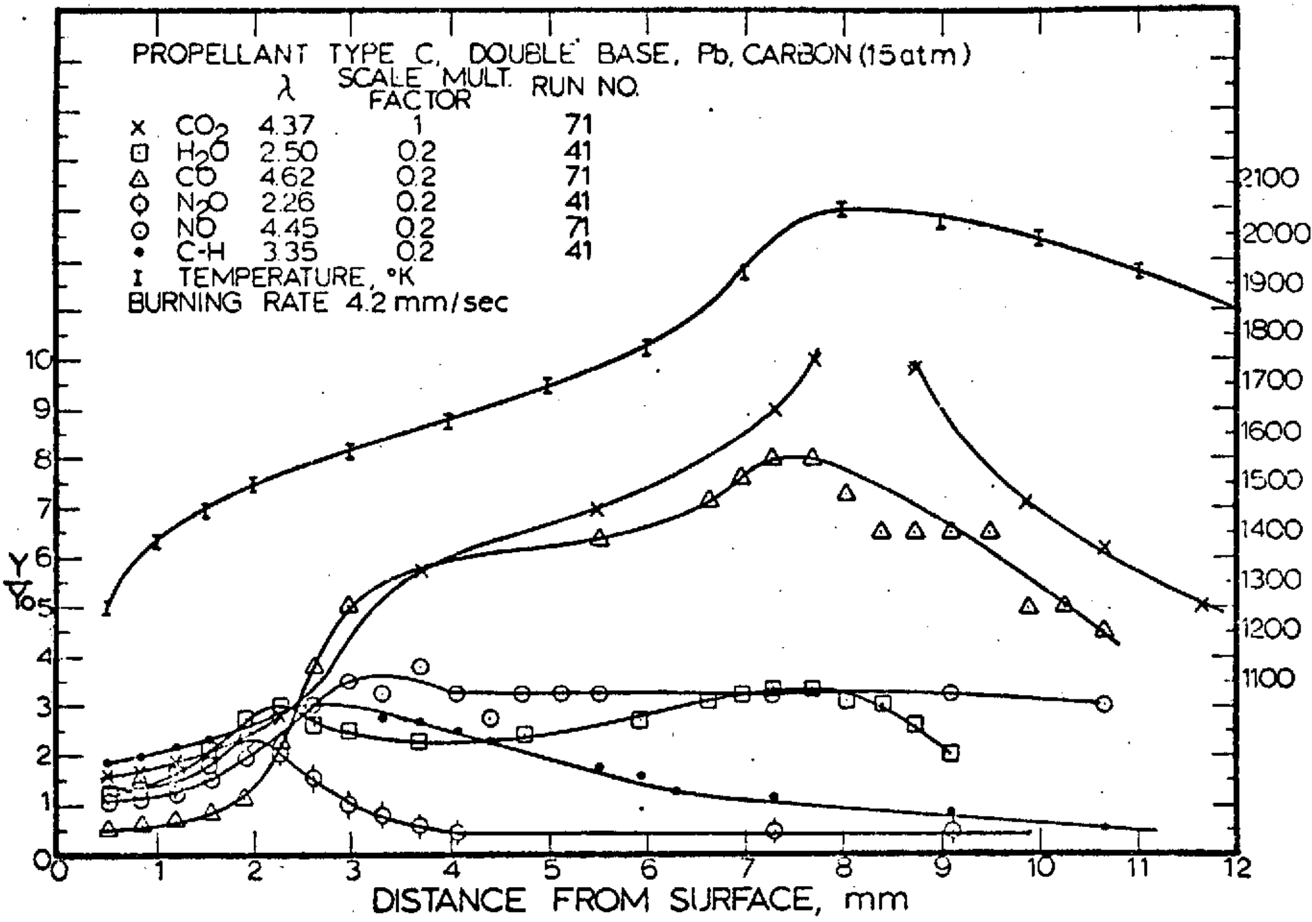

FIGURE 14. Radiation intensities from molecular species in a propellant flame are shown as a function of distance from the burning surface. This propellant is the same formulation as propellant type A (Figure 12) except it contains 0.1 percent carbon black and 1.0 percent lead salicylate.

surface. Plotted also is temperature as determined in earlier work on the same propellants [13]. Since CO_2 exhibits essentially black-body emission at 4.37 μm, its intensity follows temperature closely, at least beyond three to four mm from the surface. The exception for A propellant (Figure 12), where the CO_2 does not peak where the temperature peaks, is believed to be a resultant of a batch-to-batch variation in the burning rate.

Close to the surface, out to about 2 mm, the spectrograms do not show transmission from the source, especially in the cases of propellants A (no catalyst) and C (lead salicylate). The source signal is absorbed or scattered by particulate matter ejected from the surface. Since -CH intensity should not go through a maximum, unless the temperature gradient is much larger, it is inferred that attenuation due to the particulate matter is important between the surface and slightly beyond the position of the maximum. In that zone, temperature may be in error because particulates and gas may not be thermally equilibrated; also emission intensities may be low, because the emission received is only from the outer, cooler portion of the flame jet.

Though the spectrometer cannot reliably produce information about the chemistry of the near-surface zone, where most reaction occurs, some information can be obtained from conditions just beyond the zone and from the thickness of the zone. In the cases of propellants A and C, the final portion of -CH is consumed, though there is not enough left to affect H_2O concentration markedly; and the final portion of one intermediate oxidant, N_2O, is consumed. The principal oxidant remaining and accounting for reactions producing the last one-fourth or one-third of the total heat release may be the unknown species tentatively identified as $R\text{-}O\text{-}NO_2$.

The principal reactants in the outer part of the dark zone and in the luminous zone may be highly-condensed carbon species and possibly the unknown specie. If the oxides of nitrogen participate, it is probably as intermediates in quasi-steady state. Because this 4.85 μm peak has a high emissivity and emits as a black body, the concentration of this unknown species is not indicated by emission intensity.

For A and C propellants, the -CH emission peaks (indicating the boundary of the particulate-containing zone) appear at about the same distance from the surface, the temperature maxima likewise, even though C propellant has about twice the burning rate of A propellant. This doubling of reaction rate in the all-gas zone can be rationalized by observing that the temperature is 100 to 200°K higher. In the solid phase, however, and in the ejected particulate matter, there is catalysis by the lead. The doubling of energy supply to maintain the thermal wave is greater than the (at most) 30-percent increase in the surface temperature gradient and must be accounted for by increased rate of reactions in the solid phase. The earlier conclusion [4] that lead catalyzes solid phase reactions is supported.

The effect of copper is seen by comparing propellants A (without) and B (1-percent copper salicylate). That the peak temperature occurs at about the same distance from the surface indicates that, when the ratio of regression rates is taken into account, the overall reaction proceeds 40 to 50 percent faster in the case of B. Since the temperature is much higher, even close to the surface, suggests that the effect may be due largely to accelerated gas-phase reactions and energy feedback from the gas phase. A supporting observation is that N_2O disappears more quickly. Catalysis by copper in the gas phase is indicated. That, from visual observation, the dark zone is smaller suggests that copper may influence decomposition of the solid also.

For the B flame, -CH and NO emissions are not considered reliable; the late appearance of -CH emission is not real. The late appearance of large amounts of H_2O is significant. A difference between lead and copper seems to be that lead promotes the early appearance of H_2O, resulting in highly carbonaceous species that burn later; whereas copper promotes early formation of carbon oxides and perhaps even defers formation of H_2O.

The results of this study illustrate both the potential and limitations of the infrared spectra analysis for studying of flame reaction zones.

VII. CHARACTERIZATION OF CONDENSED-PHASE PROPELLANT REACTIONS

The development of accurate performance-predicting models for the combustion characteristics of composite propellants has required the introduction of the contributions of solid phase reaction near the burning surface. There are numerous techniques commonly employed to experimentally evaluate this contribution by a study of the pyrolysis of the solid materials, notably: differential thermal analysis (DTA), thermogravimetric analysis (TGA), or differential scanning calorimetry (DSC). All of these methods measure the bulk thermodynamic properties at relatively low heating rates, $< 1°K$ sec. Recently, high-heating-rate techniques have been developed to yield similar types of thermal information [14, 15]. Other, more specialized techniques which are utilized primarily in the study of the combustion of composite propellants or their constituents include: (a) adiabatic linear heating tests [16], (b) linear regression rate measurements [17], (c) scanning electron microscope evaluation of burned surfaces [18], (d) variations of the solid phase composition [19], (e) variations of the gas phase chemical environment, and (f) ignition characterization [20]. These and most of the other techniques yield a measure of the macroscopic influence of external parameters on the combustion processes.

An alternate approach is to consider the nature of the chemistry involved. When a chemical species characterization is required, the volatilized pyrolysis products can, in principle, be collected and analyzed. In fact, a better scheme is to analyze the changes produced in the solid phase. Infrared spectroscopy is a convenient tool to employ if appropriate samples can be obtained. Usually before and after spectra from specimens which have been pyrolized, then cooled [21, 22] are evaluated. Such methods normally utilize reflectance or perhaps absorption spectroscopy by mounting samples in salt disks or by suspension of the sample material within a salt matrix. In the present study, a direct infrared absorption technique was employed. A rapid-scanning infrared spectroscopic meter was used to obtain spectra during the heating period and as reaction occurred in the test specimens.

The radiation transmitted through a solid containing a dispersed phase is strongly affected by optical interactions at the interfaces between the two phases, and the analysis of absorption spectra for such systems can yield unique information concerning the interfacial reactions. Such a consideration was the motivation for a study of the insitu reactions at high temperatures of finely-divided ammonium perchlorate with polymeric fuel binders by use of the fast-scanning spectrometer. As part of this work, tests were made with the unloaded polymer. Analysis of these tests disclosed several interesting aspects of the pyrolysis of polyurethane-bond-containing polymers and of the value of infrared spectrometry in the study of polymer and propellant pyrolysis.

One of the major problems encountered in this study was to obtain radiation from an infrared radiation source of sufficient intensity to pass through the solid films and drive the spectrometer. It was necessary to construct a high-temperature, infrared source. An electrically-heated vitreous carbon element, which could be operated at 2700°K for several hours was used as this radiation source.

Apparatus and Procedure

The basic analytical tool employed in this investigation was the Warner and Swasey, Model 501 Fast-scanning Spectrometer. Since this instrument has been described earlier, the discussion here will be confined to outlining the operating conditions and to explaining specific modifications to the instrument. The general apparatus layout is shown schematically in Figure 1.

In this study a Perkin-Elmer Model 237 Dual Beam Spectrometer was used extensively for spectral calibration and identification.

High Temperature Source

Early in the investigation, it was determined that the available infrared source did not produce infrared radiation at a high enough intensity to yield useful signals after passage through a polymer film. This source unit was modified by replacing the silicon-carbide element with a 1/8-inch diameter vitreous carbon rod. This rod was mounted in the water-cooled holder. The carbon rod was held between copper electrodes and electrically heated. Because of expansion of the rod at the high operating temperatures, the lower electrode clamp was floated in a water-cooled, mercury-filled well to permit expansion while maintaining electrical contact. The lower copper terminal was plated with nickel to prevent amalgamation by the mercury. The rod was operated at 2750°K in an argon atmosphere, although operation at 3200°K was feasible for short periods of time. A more detailed characterization of this high temperature infrared radiation source unit is presented in reference [24].

Sample Mounting and Heater

The films to be tested were sandwiched between two 25.4-μm thick by 1.27-cm wide by 5-cm long Nichrome V strips. Figure 15 shows this arrangement. The center portion of each strip (0.5-cm wide by 2.0-cm long) had been machined away to give a window through the metal strips for passage of radiant energy. A .001 cm diameter chromel-alumel thermocouple was included in the sandwich with the junction 1 to 2 mm from the edge of the slot in the metal strips. The sandwich was then clamped between copper electrodes and placed in the common focus of the source and received units of the spectrometer system.

The output from the chromel-alumel thermocouple between the nichrome strips was used as a control system feedback signal and was recorded to yield the sample temperature history. The 0-5 ma output signal from the temperature controller was fed into a saturable core reactor (SCR) which supplied the electrical current to the sample mount and heater through a 10 to 1 stepdown transformer. The SCR and gain was adjusted to set the maximum voltage supplied to the heater to limit the heating rate. Typical temperature histories for a run in which the strip was heated to a predetermined temperature in a controlled mode and for a ballistic or uncontrolled mode are shown in Figure 16. Because the SCR unit did not have a true zero setting, initially a small current flowed through the strips, and the heating started from a temperature slightly above room temperature.

The temperature record was initially displayed with the spectral records

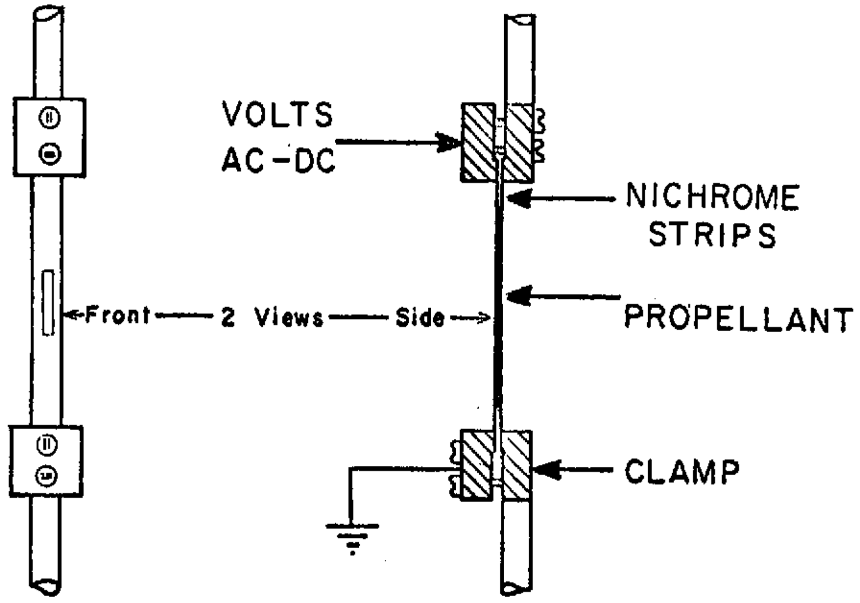

FIGURE 15. The mounting arrangement of the 25- to 50-μm thick films of propellant-like material between 25-μm thick Nichrome strips. Radiation was passed through the 250-μm wide strip indicated in the left drawing.

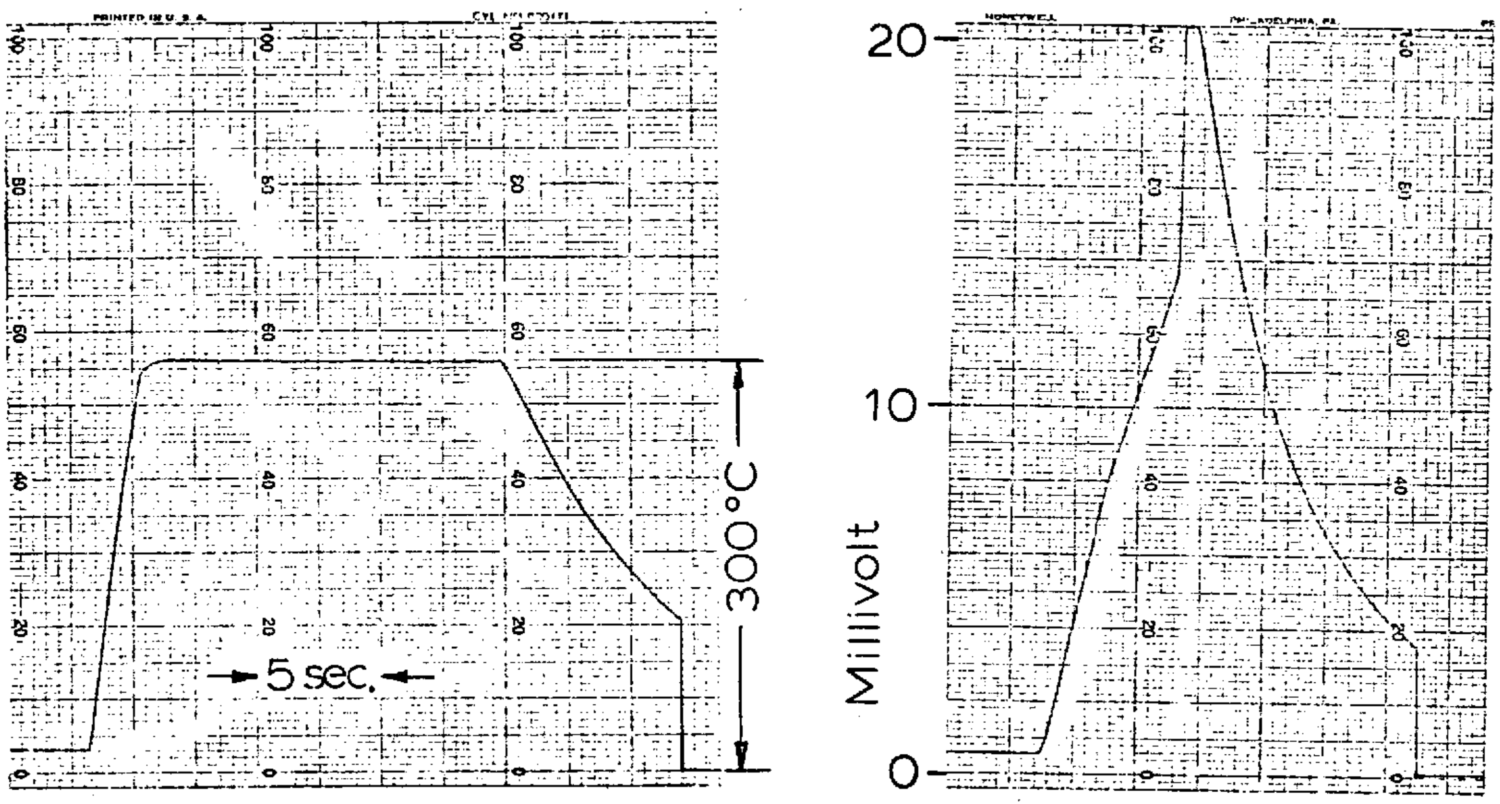

FIGURE 16. Typical thermocouple records of the strip temperature for the two types of tests employed in this study. On the left is a record from a test in which the temperature was controlled at 598°K after initial heating. The record on the right was obtained from a test in which the film was heated at a constant energy input rate to ignition. The time and temperature scales are the same for both plots.

on an oscilloscope face, but in later tests the temperature was recorded on a strip chart recorder. The accuracy of the transient thermocouple reading was checked by a remote sensing, infrared thermometer and the two temperature measurements were found to agree to within ±3°C. The SCR output was also recorded by the oscilloscope, along with the spectra, in order to relate the strip chart record with the spectral scans records.

Spectrometer Operation

Spectra were obtained at the 8-per-second rate with the spectrometer. The 2.5- to 5.5-µm range of the spectrometer, which employed a liquid nitrogen cooled Indium Antimide (InSb) detector, was used almost exclusively in this study. Some tests were run with the 5.5- to 9.0-µm range which required a liquid helium cooled copper doped germanium detector. Because of the low transmission levels, information obtained at longer wavelengths was not very useful. The entrance and exit slits of the spectrometer were set at 0.50 mm.

Spectral Recording

The output signal from the spectrometer was displayed as one dot on the face of a Textronics Model 561 Oscilloscope, and the oscilloscope was operated without a time base. A signal trace was generated and recorded on 35-mm film with a Beattie-Coleman KD-5 Oscillotron camera. The camera was operated as a strip camera at a speed of 8 inches per second. Movement of the film produced the time (wavelength) scale. Each of the 24 scan-wheel corner mirrors of the spectrometer was observed to yield a slightly different signal for the same source intensity. The scan wheel mirror which yielded the lowest magnitude was chosen as Mirror 1 since it could be easily identified under all conditions, and all spectral outputs were corrected for mirror differences.

A fixed-focus-microfilm reader was used to evaluate the data from the

35-mm film. The various peak heights were read manually by use of moveable scales.

Operating Procedure

The polymer-film-nichrome-strip sandwiches were mounted on a machinist's table. The slot in the strip position was moved within the focus to maximize the output signal from the spectrometer while operating the infrared source unit. The sample heating rate was determined by selecting the maximum voltage from the control system while the reaction temperature was determined by adjustment of the set point on the controller. The magnitude of the initial heating rate was limited by the requirement that the control system not yield an overshoot of the final reaction temperature (see Figure 16). After the operation of the spectrometer and the recording systems were stabilized, the electrical power was applied to the metallic-strip-polymer sandwich. Spectra and the applied voltage were recorded on 35-mm film, prior to heating, during the temperature rise, during 10, 30 or 60 seconds at the control temperature, during part of the cool-down period after cutting off of the electrical current, and later after the sample had cooled to room temperature. The temperature was recorded on a strip chart recorder and was later related in time to the 35-mm spectral record by use of the initial indication of the heater voltage on the 35-mm record. Normally, the film from a test was removed from the slot by either cutting away the films after a test or as the result of ignition and burning of the films. The signal transmitted through the cleared slot was used as the total transmittance base curve during the data analysis. In some cases, the films were not destroyed so that absorption spectra before and after heating could be obtained with the dual-beam Perkin-Elmer spectrometer. In several tests, the films were subjected to repeated temperature cycling; while in others, the films were heated to their ignition points. All tests reported in this study were conducted in air at 0.85 atm. For the test times of interest here, the data of Bouck [14] indicate little air-polymer reaction for this system below 700°K.

During the transient heating period, the temperature difference ΔT_m between the metallic strips and the center line of the exposed film near the maximum temperature could be approximately given as [23]

$$\Delta T_m = \frac{r}{2}\,\frac{\ell^2}{K} \quad . \tag{1}$$

In this study, the heating rate employed, r, and the half slit width, ℓ, were respectively, $r \cong 80°C/sec$ and $\ell = 0.025$ cm. For a thermal diffusivity typical of such films of $K \cong 1.2\times10^{-3} cm^2/sec$, the ΔT_m would be approximately 2°C during heating. Once at temperature, ΔT_m would differ from zero principally as a result of radiant heat loss from the films. At about 600°K for a 25-µm thick film, this temperature difference would be nearly 30°C. However, a significant amount of radiation from the 2750°C focused source was absorbed in the films, and the strip to centerline temperature difference was therefore somewhat less than this value. It thus appears that the reported thermocouple temperatures are likely higher than the true average film temperature by about 10±5°C, and that the greatest temperature difference across the surface of the exposed films was 10 to 20°C at the highest test temperature.

Preliminary Considerations

As in most experimental projects, the initial results point up the deficiencies of the apparatus and procedures, define certain objective limits, and indicate the extent of experimental testing requirements. The preliminary results obtained at the start of this program were used to: (1) outline the requirements for the materials that could be studied with the proposed experimental techniques, and (2) aid in the selection of the types of tests needed to achieve the objectives of this study.

Material Selection

The determination of the best propellant fuel-binder to be mixed with ammonium perchlorate (AP), to yield test films, required considerable effort. The selection of an elastomer was based on the following criteria: (1) a commercially available material of current interest as a fuel-binder was desired; (2) thin, 25- to 50-μm thick, films could be produced which had adequate physical integrity, with or without solid loadings, to withstand heating to the ignition point; (3) the infrared spectra of the polymer had to be simple enough to permit identification of important absorption bands characteristic of both the polymer and AP; (4) infrared windows or grey absorption regions near the spectral absorption band had to be present to permit evaluation of band absorbances from the spectra of the single-beam spectrometer; and (5) the procedure for preparation of films at various AP loadings had to be relatively simple.

Some of the binders tested are listed below along with the reasons why they were discarded:

1. PBAA-EPON 828 (Polybutadiene acrylic acid co-polymerized with Shell-Epon 828). In this material, the spectral region near 2.74 μm, which was required as a window region in the data reduction method, was masked by the influence of the polymer bonds in that region.

2. Polyurethane (B. F. Goodrich Estane with Thiokol JR C7 curative-1). It was not possible to prepare films of 25- to 50-μm

thickness by the methods tried, with or without AP. Also, this elastomer had a tendency to melt prior to ignition.

3. PMMA (Polymethyl methacrylate). This was not a fuel-binder of current interest, and the films melted before any significant reaction occurred.

Several other propellant combinations were available in the cured or ingredient form but were eliminated because of failure to meet the requirements stated above.

The majority of the tests performed in this study were made with a solid elastomer which contained 92.5 weight percent hydroxyl-terminated polybutadiene (ARCO Chemical Co. R-25, functionality 2.2-2.3 and 0.85 meg OH/gm). This material was crosslinked or extended by forming a urethane group with 7.5 weight percent isophrone diisocyanate (PIDI). The solid elastomer is normally referenced as the HTPB fuel-binder. This particular combination met all of the criteria stated above. The spectral character of this material in the 2.5 to 5.5-μm region is quite simple. The thin films of this material displayed excellent adhesive properties, thus insuring a good thermal contact with the heating strips.

Fine ammonium perchlorate of 5-μm particle size was used to obtain several particle thicknesses through the 25-μm thick films. The thickness of the films and the quantity of AP added to the films were selected to give about equal absorption of the 3.04-μm NH band of the AP and the 3.42-μm CH band of the binder. Normally, 30 weight percent of AP was used. A standard propellant formulation generally contains 70 to 80 weight percent AP, but at this high loading, most of the binder absorptions were masked by the nearly black AP absorption bands. A typical spectra is shown in Figure 17 and illustrates the two absorption bands of interest. It was found that film

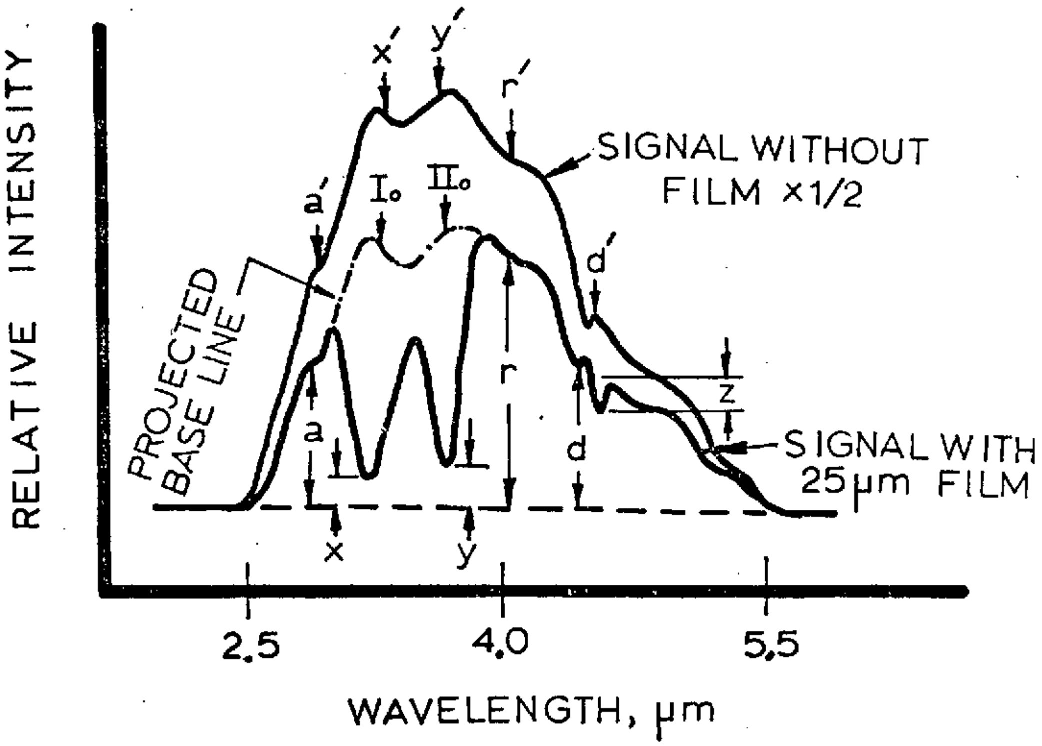

FIGURE 17. A sketch of the output from the single-beam fast-scanning spectrometer is shown here. The 2.5- to 5.5-μm range was scanned in 0.1 second. The symbols on this plot are interpreted as:

a - 2.4 microns, window used in rapid-scanning baseline reduction method,

x - 3.04 microns, NH absorption due to NH_4ClO_4 in a loaded polymer; a window for HTPB-polymer,

y - 3.42 microns, CH absorption of polymer materials,

r - 4.03 microns, window used in rapid-scanning baseline reduction method,

d - 4.38 microns, window used in rapid-scanning baseline reduction method, and

z - 4.45 microns, NCO absorption of polymer materials.

thicknesses greater than 50 μm or AP loadings greater than 40 weight percent yielded essentially complete absorption at the bands of interest.

A detailed discussion of the spectral identification of the individual components and the spectra obtained from various combinations of ingredients before and after curing is outlined in reference [24] for the HTPB-IPDI-AP system. A summary of the identification results is presented in Table 1. Figure 18 presents spectra from the slow-scan, dual-beam spectrometer which shows the various bands. The absorption bands of interest here of the elastomer and the AP are identified in these figures. The position of the uncured-polymer and the reacted-film isocyanate adsorption band has been indicated. The various bands are designated by a letter and a number. The prefixed letter A designates an AP absorption band. The letter H signifies an absorption observed in pure R-45, the letter I designates an absorption traceable to the IPDI, and the letter N signifies an absorption band which appeared after curing the elastomer mix which is likely due to the urethane link.

Test Selection

This study was initiated to develop a method for obtaining kinetic information on the solid phase reactions in composite propellants. The approach was to heat thin films as rapidly as possible to various fixed reaction temperatures and to follow the changes in the infrared absorption spectra with time at the fixed temperature. Several tests were performed at the same conditions to insure data reliability. The following paragraphs outline the test groupings and define the various materials that were selected on the basis of the information gained from the preliminary tests.

HTPB-30. Fifty to sixty tests were conducted with 25-μm thick films containing 30 percent AP to obtain kinetic information. Several films were heated more than once.

TABLE 1

A Summary of the Identified Adsorption Bands

The prefixed identification letters A, H, I, and N indicate bands which associated with the ammonium perchlorate, the R-45 polymer, and the isophoronediisocyanate (IPDI), respectively.

Band	Wavelength, μm	Mode[1] (bond) notes
A1	3.04	ν(NH)
A2	4.90	(ClO)
A3	5.04	(ClO)
A4	7.04	δ(NH)
A5	9.40	ν_s(ClO)
A6	10.69	ν_s(NH) forbidden
H1	2.79	ν(OH) free
H2	2.94	ν(OH) bound
H3	3.25	ν(CH) alkane
H4	3.32	ν(CH) alkane
H5	3.42	ν(CH) alkane
H6	3.51	ν(CH)
H7	5.46	unknown
H8	6.10	ν(C=C)
H9	6.90	δ(CH_2)
H10	6.97	δ(CH_2)
H17	10.33	unknown
H18	10.96	unknown
I3	3.42	ν(CH_2)
I3	3.38	ν(CH) alkane
I4	4.45	ν(CH) alkane
I4	4.45	ν(-N=C=O)
I8	6.85	δ(CH)
N1	5.79	ν(C=O) amide I
N2	6.62	(β(NH) + ν(NC)) amide II
N4	8.16	(β(NH) + ν(NC)amide III) + ν(O=C-O-C)
N5	8.89	ν_s(O=C-O-C) + ν_a(C-O-C)
N6	9.76	ν_s(O=C-O-C)
N7	12.95	γ(O=C-O-C) amide V

---

[1] The symbols ν, δ, β, γ, correspond to stretching, bending, in-plane bending, and out-of-plane bending of the bonds.

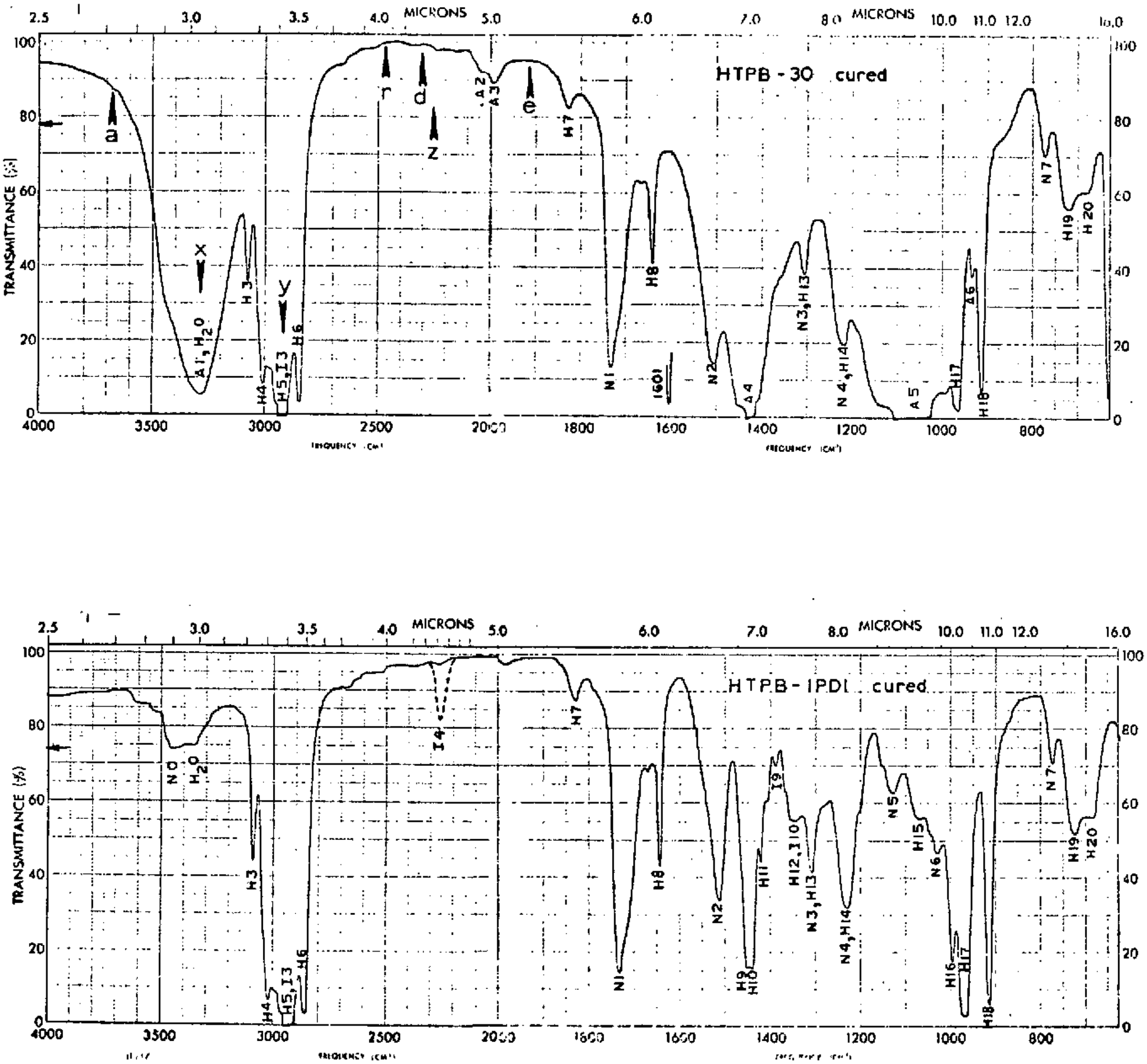

FIGURE 18. The absorption spectra of the HTPB-30 (a) and HTPB (b) films.

HTPB-50. Only a few tests were conducted with the 50 percent AP films. These tests with 25-μm thick film were made to evaluate the AP loading effect.

HTPB-50 NaCl. These HTPB films contained 50 percent fine sodium chloride. These films were tested in order to evaluate the optical effects of solid-elastomer-surface interactions and the check for possible elastomer reactions. The 50 percent NaCl loading was used to produce a film comparable in volumetric loading to the 30 percent AP films.

HTPB-IPDI. The elastomer only tests were performed on 50-μm cured films. Cured films of less thatn 50-μm thickness could not be handled nor transferred onto the nichrome heating elements.

PBAA-30. For comparative purposes, tests were run with films of the polybutadiene-EPON 828 co-polymer containing 30 percent AP.

Several of the HTPB-30 and the HTPB-IPDI samples which has been heated and tested at the focus of the fast-scanning spectrometer were recovered, and their infrared absorption spectra was obtained by use of the dual-beam, slow-scan spectrometer. These films were not destroyed, as was the normal procedure for rapid scan tests where a full transmittance baseline was required.

Data Reduction

The large quantity of information generated with the fast-scanning spectrometer during each test required a data reduction technique that would correct for the aspectral variations yet retain the important spectral features. The reduction approach used in this study was to first determine the behavior of the aspectral absorption regions as the films were heated. The desired spectral intensities were then determined by use of a baseline established from the adjusted aspectral regions. Assuming then that the most critical features of the spectra were thus known, the mirror corrected spectra absorption data were converted into fractional concentrations by use of the Beer-Lambert law.

Calculation of Absorbances

A difficulty which must be considered when interpreting the spectral output from the single-beam, fast-scanning spectrometer is the establishment of the aspectral intensities at the wavelength of band absorption. The problem is solved on a dual-beam instrument by simply increasing the electronic gain to produce a "100 percent" transmission signal at "window" regions. In the case of a single-beam instrument, it is necessary to establish a baseline for the signal for no spectral absorption at the wavelength of interest. The absorbance, which is defined as $A = \log_{10} I_0/I$, is required. In the typical single-beam spectra signal shown in Figure 17, the intensities, I, of the -NH and -CH bands are proportional to x and y respectively, and the aspectral intensities, I_0, for the same wavelength are I_0 and II_0 respectively, in this figure. The projected baseline curve in Figure 17 is obtained from the spectral signal without a film in the sample mounting scaled to produce the same signal intensities at a, r, and d, the window regions. A wavelength dependent scaling factor must be used. The form of this dependence and justification for its use are presented in reference [24].

Beer-Lambert Law

The Beer-Lambert Law can be used to convert the measured signal intensities of x and y with the calculated baseline intensity projections of I_0 and II_0 to values of concentration. The Beer-Lambert Law, written for the NH bond in AP, is,

$$A = \log_{10} \frac{I_0}{x} = \varepsilon C_x \ell \quad ,$$

where

ε = coefficient of absorption or molar extinction coefficient, ℓ/gmole-cm, and

C_x = NH bond concentration, gmole/ℓ.

In most cases, the data presented here are in terms of absorbances since not all of the deviations from the Beer-Lambert Law were considered. If one assumes that the thickness of a film does not vary and that ε is constant, the absorbances would be proportional to the concentrations of the various bonds.

Experimental Results

If, for the AP-HTPB system of interest here, the coefficient of absorption, ε, in the Beer-Lambert Law were independent of temperature, it would be possible to relate infrared absorption measurements to species concentrations as the film was heated to the ignition temperature. Tests were conducted with such an intended objective, and the results of these tests will be discussed later. However, it was found that not only was the coefficient of absorption not a constant, but that the transmissivity of the films, even at the window regions, was a complex function of temperature. In the following paragraphs, the observations concerning the effect of temperature on infrared absorption in the various types of films is discussed.

At a constant temperature, the absorption coefficient was apparently constant. It was thus possible to make a valid interpretation of tests in which the films were quickly heated to a preselected temperature and the reaction of the AP and polymer was followed by noting the changes in the absorbance at the 3.04-μm (NH) and 3.42-μm (CH) wavelengths. A discussion of these tests and the presentation of the results in terms of conventional reaction kinetic notation are made in the last part of this section.

Optical Effects in the Sample Films

Figure 19 is a presentation of typical results from a test on a 25-μm thick film of HTPB containing 30 percent AP. This film was heated at a rate of 80°K/sec to 590°K and held at this temperature for several seconds. Essentially the same results were noted with films of the PBAA fuel-binder. The transmitted signal intensities are plotted as a function of time. The intensities are the heights measured from the spectral signals at 4.30 μm (r) and 2.74 μm (a), the window regions cited in Figure 17, and at the NH and CH band absorptions of 3.04 μm (x) and 3.42 μm (y), respectively.

The effect of increasing temperature is to increase the infrared transmittance at all wavelengths. A similar effect for visible radiation was noted by Mihlfeith [25]. At about 513°K, the temperature of the orthorhombic to cubic phase change for AP, a decrease in the transmittance or signal intensity was noted. This decrease is likely the result of the changes in crystal density and orientation in the film. As the temperature was increased above 513°K, the signal intensities again increased at each wavelength. Once the film reached a constant temperature, the signal intensity at the window regions (4.30 and 2.74 μm) decreased slowly with time as the film darkened at the high temperature. The signal intensities at the NH and CH bands would increase, decrease or remain relatively constant, as in FIgure 19, depending on the relative rates of the film darkening and the rates of the oxidizer-polymer reaction. As discussed earlier, the absorbance, A, at any time, was related to the values of both the signal intensity at the window regions and at the absorption bands.

The decreases in the magnitude of the transmitted radiation intensity through films at 513°K and after reaching the preselected temperature are easily explained in terms of the arguments presented above. The explanation

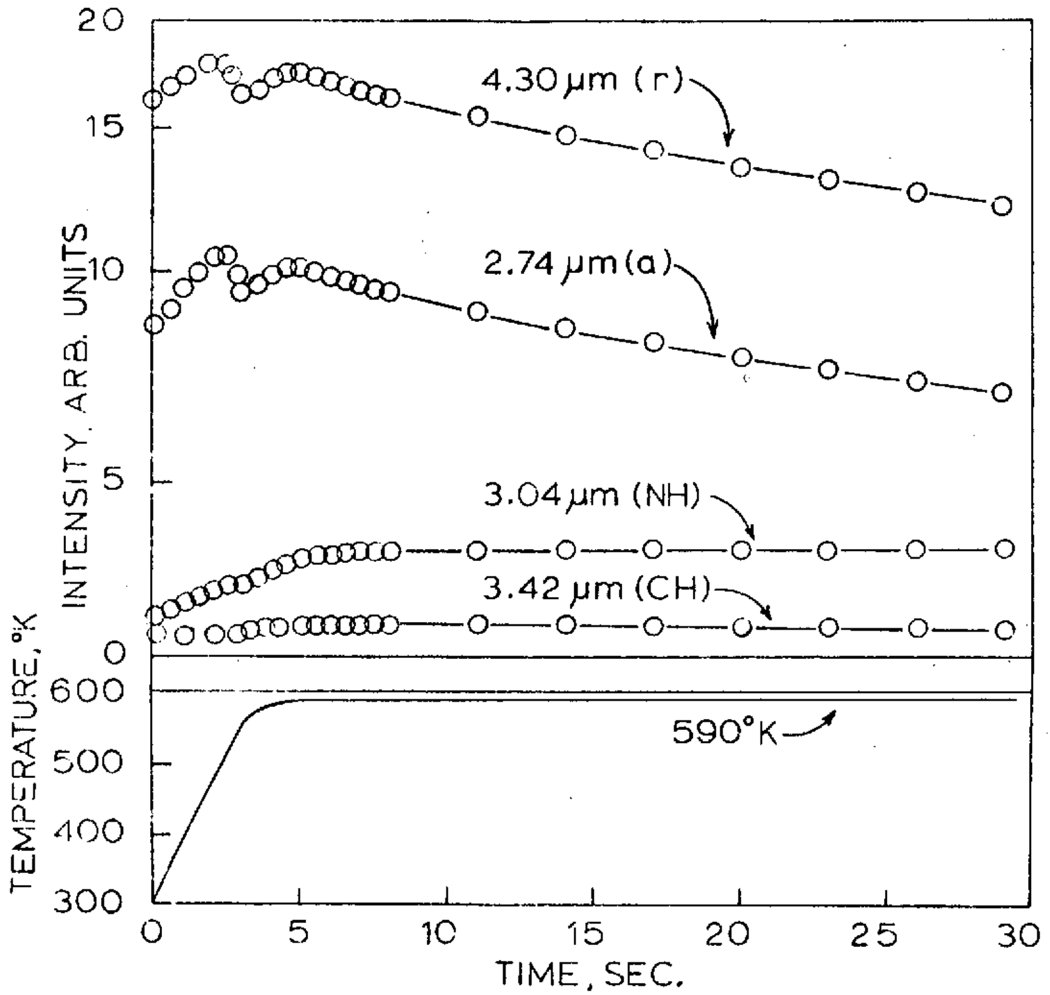

FIGURE 19. The magnitude of the signals (intensities) at the various wavelengths measured as indicated in Figure 17 are shown here as a function of time and temperature for a test on a 25-µm thick film containing 30 percent AP in the HTPB fuel-binder.

of the increase in the transmitted signal intensity with increasing temperature is more complicated. The possibility of this effect being strictly a phenomenon of the HTPB was checked by making tests on unloaded films of polymer. Figure 20 presents the results of such a test on a 50-μm thick HTPB film which was heated to 625°K. In this case, the transmission of radiation was dependent on temperature although the dependence was different from that of the AP loaded films. When the same film was reheated, it was found that the transmissivity of the film was essentially constant with temperature. It was postulated that the effect noted in Figure 20 for the HTPB film was the result of inhomogeneous regions in the polymer of a size comparable to the wavelength of the light. These regions appear to disappear after heating the film. The pyrolysis of the polymer has been studied by this technique, and the results of these tests are presented in references [24] and [26]. Unfortunately, the effects illustrated in Figure 19 for the AP-loaded films were still observed with reheated films.

An additional test was made in an attmept to characterize the peculiar dependence of loaded film transmissivity on temperature. Films of the HTPB polymer were prepared which contained 50 percent of very fine sodium chloride. Figure 21 shows the results of a test with a 50-μm thick film heated to 620°K. In this case, the film transmissivity decreases as the film is heated. It thus appears that an effect was observed which was dependent on a polymer-crystal interaction. This optical interaction likely occurred at the interface of the two phases, which suggests that the interfacial reaction was characterized by the absorption technique used in this study.

Characterization of AP-HTPB Reaction

Figure 22 illustrates the type of results obtained when an AP-containing film was heated to its ignition temperature. The NH and CH absorption is

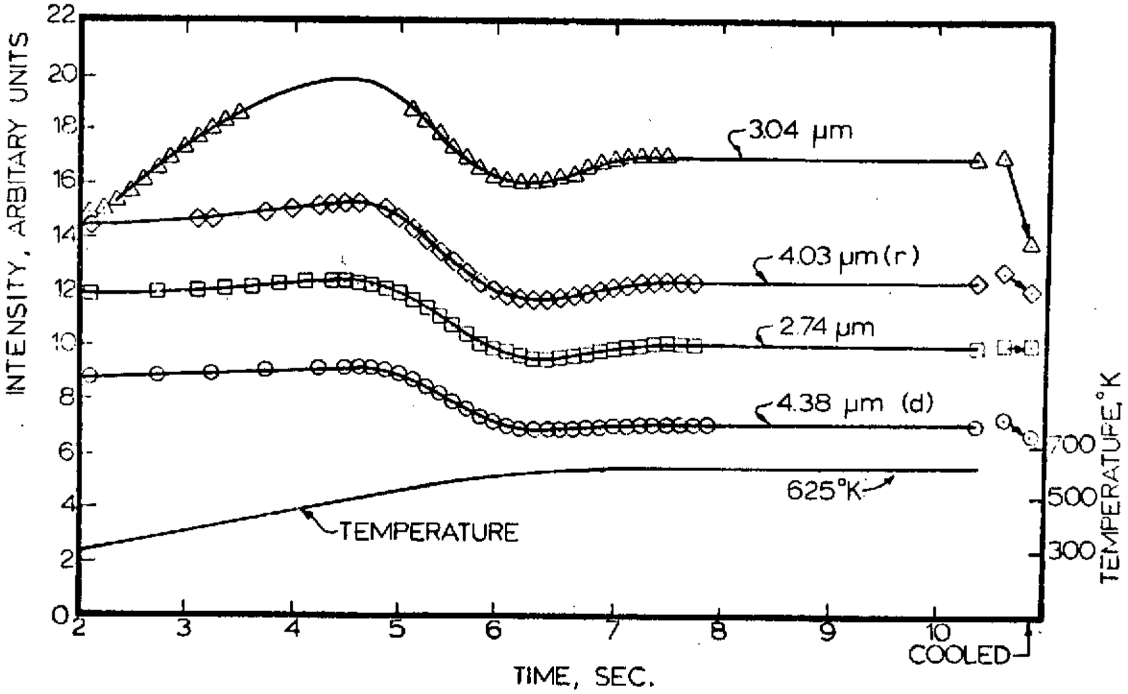

FIGURE 20. The measured intensities for a test with a 50-µm HTPB film at the several window wavelenghts indicated in Figure 17 as measured with the rapid-scanning spectometer as a function of time and temperature. The last two symbols on the right correspond to values after 60 seconds and after cooling to near room temperature, respectively.

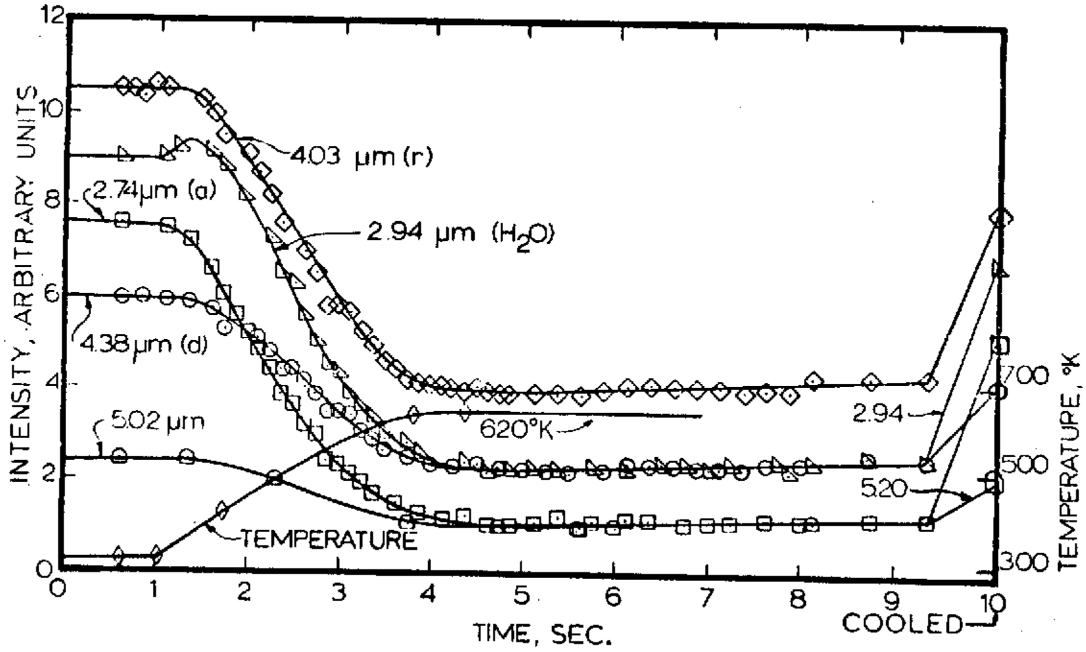

FIGURE 21. The intensities measured during a test with a 50-µm thick film of HTPB containing 50 percent fine NaCl as a function of time and temperature.

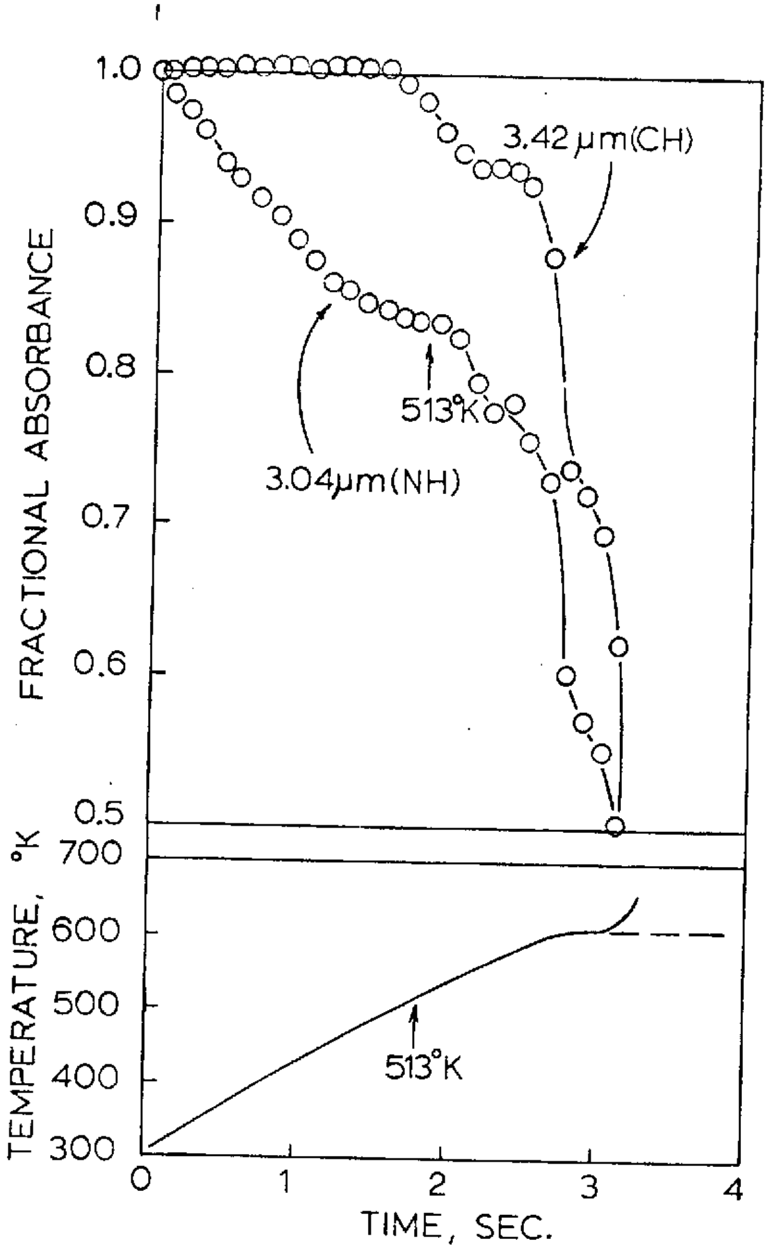

FIGURE 22. The fraction absorbances at 3.04 μm (NH) and 3.42 μm (CH) are shown here as a function of time and temperature from a test with a 25-μm thick film of HTPB-30 heated to ignition.

presented in terms of a fractional absorbance, i.e., the ratio of $\log_{10}(I/I_0)$, at any time to the value at the start of heating. If the Beer-Lambert Law were applicable and the absorption coefficient, ε, were independent of temperature, a plot such as Figure 22 would be interpreted as a plot of fraction unreacted of the species as a function of time. The decrease of the NH absorbance with temperature at temperatures below 500°K illustrates the incorrectness of this assumption in this case. For temperatures less than 500°K, it is unlikely that a significant fraction of the AP reacts at the heating rates employed in this study. Either the absorption coefficient at 3.04 μm is strongly temperature dependent, or more likely, bound water (which also absorbs at 3.04 μm) was being eliminated from the film. The behavior of the pure polymer film transmissivity at 3.04 μm illustrated in Figure 20 tends to support the absorbed water postulate. In contrast, the CH band absorbance remained constant up to 500°K. The Beer-Lambert Law may be applicable to the CH band for the temperatures considered here.

In most cases, the NH band absorbance appeared to become constant just as the temperature of the AP phase change was reached. Figure 22 illustrates this effect. At about 513°K, both the CH and NH absorbances decreased rapidly. For the test cited in Figure 22, the intended constant reaction temperature was to have been 603°K, but apparently the effect of the exothermic reaction in the film was great enough to dominate the energy balance and ignition or destruction of the film occurred. A fraction absorbance of about 0.2 for both the CH and NH bands was measured just prior to disappearance of the film. Figure 22 is a semi-quantitative history of the species concentrations and film temperature during the early ignition transient.

A comparison of the results shown in Figure 22, which was derived from a test with a 30 percent AP-loaded film at a controlled temperature of 603°K, to the data in Figure 20 for a pure polymer film at 625°K, leads to an important conclusion. Little decomposition of the polymer occurred at temperatures less than 625°K for the test times of interest here. However, in the presence of the ammonium perchlorate, rapid disappearance of the polymer occurs at temperatures below 600°K. It appears that the reaction under study is the interaction reaction between AP and the HTPB polymer, and at least partial oxidative pyrolysis of the binder occurred. The results of the high heating rate tests of Bouck [14] on this same system support this observation.

Figure 23 shows a typical result, as a short time and longer time history, from a test of a 25-µm thick HTPB-30 film heated at 80°K/sec to (and held at) 590°K. Here, and in all subsequent discussions, time is measured from the start of film heating. Again, as seen in Figure 22, the CH band absorbance was constant and the NH band absorbance decreased as the temperature rose to 513°K. At the phase change temperature, both absorbances then decreased. In this case, when the film was maintained at a constant temperature of 590°K, both the CH and the CH band absorbances decreased monotonically with time. The film absorbances after cooling are shown at the right-hand side of the long-time scale plot. The agreement between the last high temperature measure value of the CH absorbance and the room temperature value illustrates the apparent constancy with temperature of the Beer-Lambert law absorption coefficient for the CH band. A significant change in the NH band absorbance after cooling was noted however.

If the room temperature values of the fractional absorbances are assumed to be equal to the fraction of the unreacted AP and HTPB (treated here as C_2H_3), it is possible to evaluate the ratio of AP to HTPB reacting in the films. From Figure 23, values of 0.16 and 0.48 are obtained for the reacted

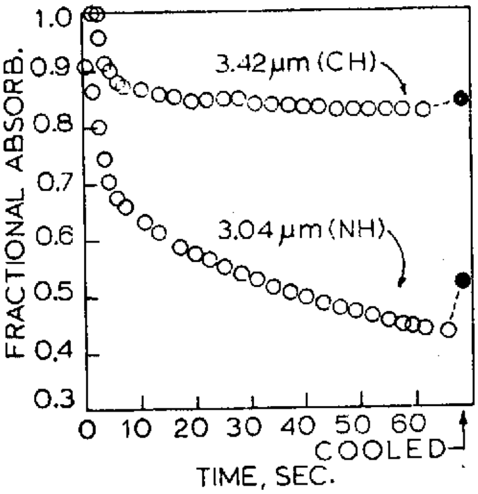

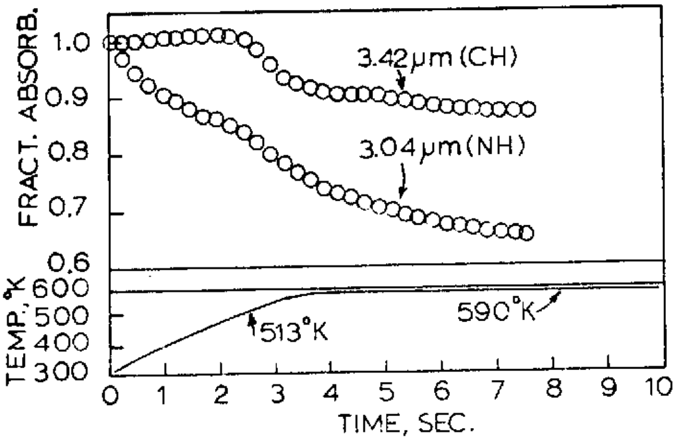

FIGURE 23. Typical short and long time histories of the CH and NH fractional absorbances as a function of time and temperature. Cooling of the film started at 65 seconds. The darkened symbols on the right of the plot correspond to the room temperature fractional absorbances of these bands after cooling the reacted films.

fractions of NH and CH. These numbers yield a ratio of 0.77 gram polymer per gram AP reacted. On a molar basis, this ratio would indicated 3.4 moles of C_2H_3 were lost per mole AP reacting; these are typical values for most tests. Thus, considerably more polymer was consumed than the stoichiometric ratio of 0.714 for reaction to CO and H_2O.

If the Beer-Lambert law is applicable at constant temperature, a fractional absorbance plot such as Figure 23 would be effectively a plot of fraction of the species (HTPB or AP) unreacted as a function of time, and conventional techniques for evaluating reaction kinetic parameters would be applicable. The validity of this law for this system at room temperature was checked by use of films containing various amounts of the oxidizer crystals. However, there appears to be no was to check this law at the high temperatures of interest here.

In the case of the NH band, the fractional absorbance does not equal the fraction unreacted; only changes at constant temperature are related. Since only changes in NH concentrations could be measured, the absorbance data could only be interpreted in terms of first order reaction kinetics. Fortunately, for total times greater than 10 seconds, the plot of the rate results yields a straight line as the logarithm of fractional absorbance (or unconverted) versus time, and the first order kinetic model is a good representation of the experimental data. Figures 24 and 25 present the results in this form for ten tests conducted between 560 and 616°K for the NH and CH bands respectively. The first order reaction rate constants derived from the lines in Figures 24 and 25 are summarized in Table 2 and are plotted in an Arrhenius-type plot as a function of temperature in Figure 26.

Although there is considerable scatter in the data shown in Figure 26, it is apparent that the NH reaction is considerably faster than the CH reaction.

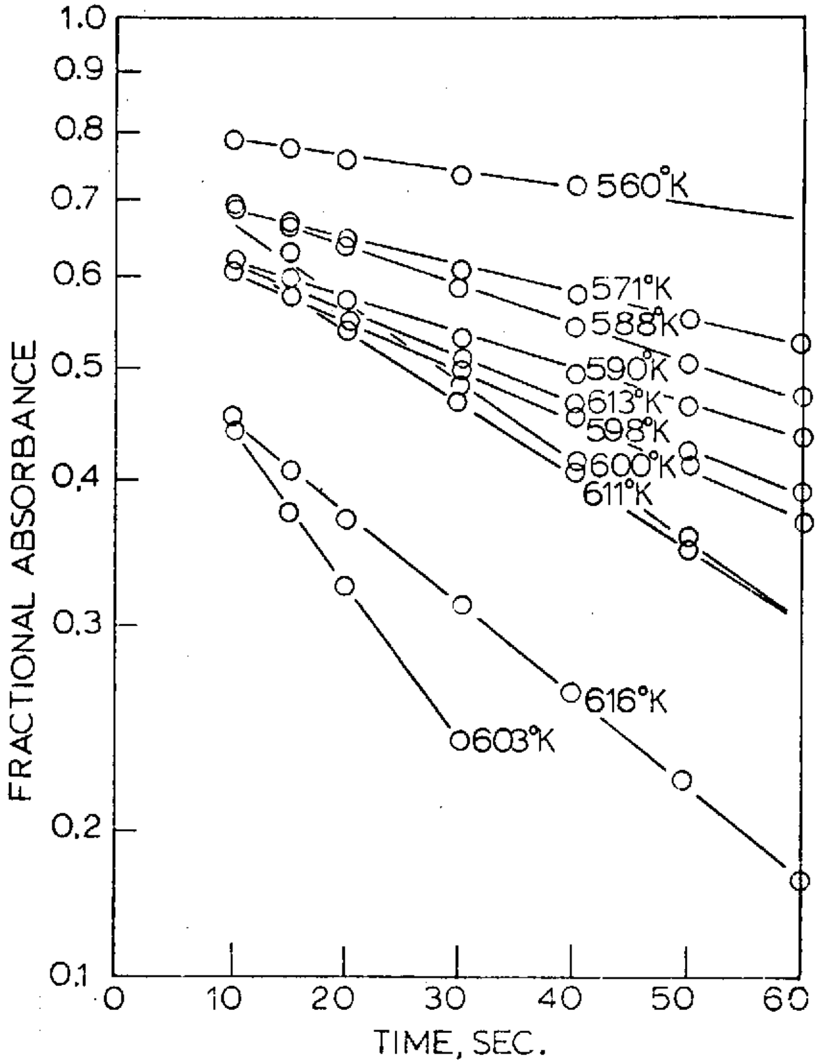

FIGURE 24. A semi-logarithmic plot of the fraction absorbances of the 3.04-μm NH band as a function of time for several tests of 25-μm thick HTPB-30 films at various temperatures.

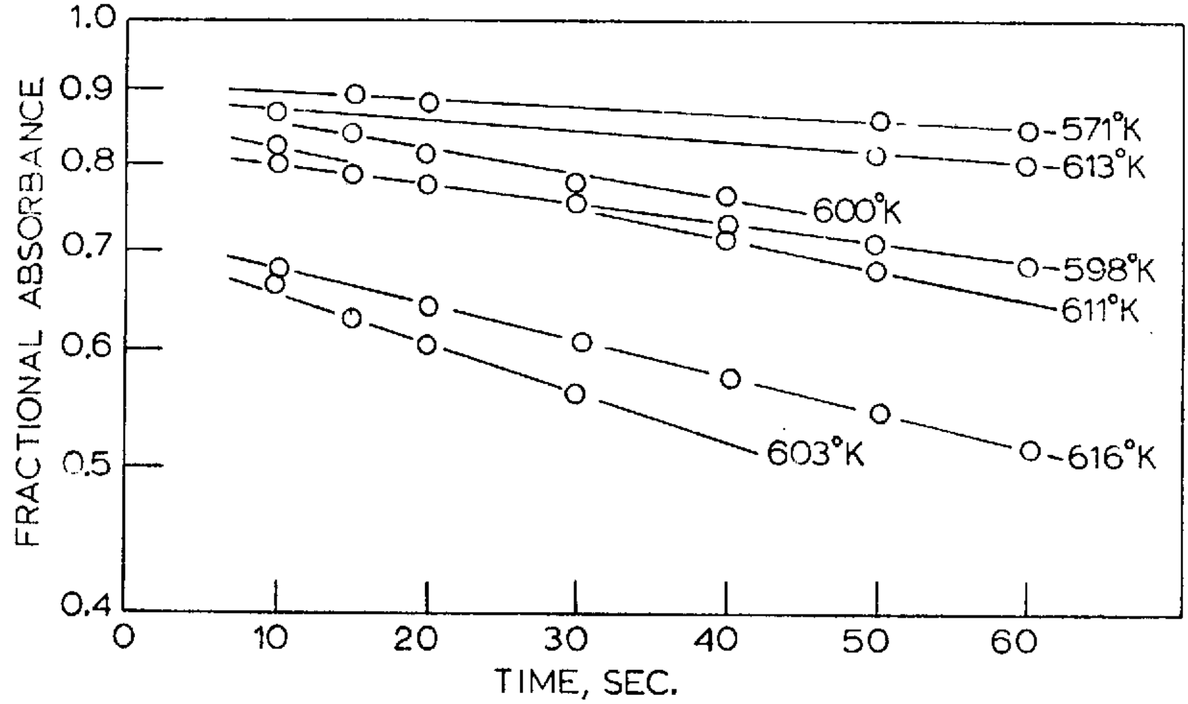

FIGURE 25. A semi-logarithmic plot of the fraction absorbances of the 3.42-μm CH band as a function of time for several tests of 25-μm thick HTPB-30 films at various temperatures.

TABLE 2

A Summary of the NH and CH First-Order Reaction Rate Constants for Total Times of 10 to 60 Seconds

Temperature, °K	Reaction Rate Constants, sec^{-1}	
	NH Band	CH Band
560	3.18×10^{-3}	1.23×10^{-3}
571	5.41×10^{-3}	1.26×10^{-3}
588	9.01×10^{-3}	1.97×10^{-3}
590	7.44×10^{-3}	$.911 \times 10^{-3}$
591	9.05×10^{-3}	1.29×10^{-3}
598	8.62×10^{-3}	3.92×10^{-3}
600	17.1×10^{-3}	4.18×10^{-3}
603	30.7×10^{-3}	8.39×10^{-3}
611	14.5×10^{-3}	4.82×10^{-3}
612	18.1×10^{-3}	5.48×10^{-3}
613	9.18×10^{-3}	1.44×10^{-3}
616	18.1×10^{-3}	5.53×10^{-3}

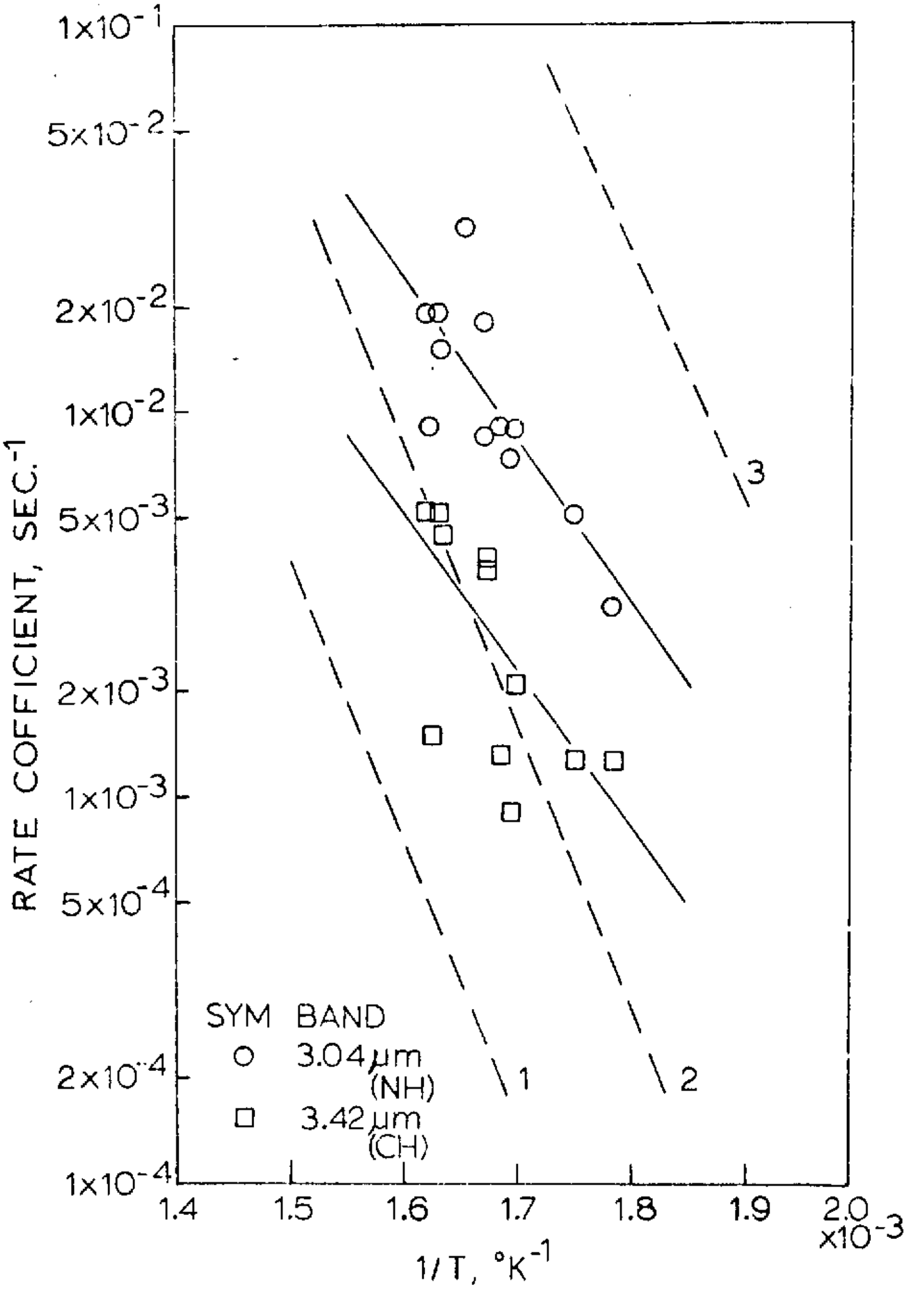

FIGURE 26. An Arrhenius plot is shown here of the first order rate constants derived from the data in Figures 24 and 25 and summarized in Table 2. The solid lines are the least squares representations of these data. The dashed lines labeled 1, 2 and 3 are derived from data presented in references [28], [16] and [20] respectively.

The reactions were, however, apparently coupled; the correlation coefficient between the two sets of rate constants is greater than .93, which is much greater than the correlation of the rate constants with temperature.

A comparison of these kinetic data to published values for the decomposition kinetics of AP and propellants is of some interest. The considerable quantity of kinetic data summarized by Jacobs [27] on the AP decomposition reaction is really not comparable to the results presented here. Although both types of tests were conducted at temperatures above the phase change temperature, the time scale of the measurements and the observed reaction rates at the same temperature differ by about two orders of magnitude. The conventional laboratory tests were simple not studying the reaction of interest here.

The results of three studies have been presented which can be compared to these data if some reasonable assumptions are made. Figure 26 presents the comparison. Waesche [28] presented data from DSC tests on various propellants; Inami, Rosser and Wise [16] made adiabatic heating tests on slabs of propellants; and Baer and Ryan [20] conducted hot-wire ignition tests on several propellants. Each summarized their data in terms of kinetic constants. Two adjustments to these published results were required to produce the comparison shown in Figure 26. Since the interpretations of the thermal and ignition tests yielded pre-exponential factors in terms of energy release rates rather than as a rate constant, it is necessary to estimate the thermal energy yield of the reaction to obtain a comparable pre-exponential factor. A value of 131 kcal/g-mole of AP reacted was assumed here, which corresponds to reaction of the AP and HTPB polymer to CO, H_2O, N_2 and HCl. Also, since the tests reported were on propellants containing 75 to 80 percent

AP, it was necessary to use a correction factor for comparison to the 30 percent AP films. The published pre-exponential constants were simply multiplied by the ratio of AP concentrations in the two cases. Because of these approximations, the lines for prior published results in Figure 26 are only estimates. Nevertheless, it appears likely that the same reaction was considered in each case.

The prior studies cited all report an activation energy of about 30 kcal/g-mole. The least squares fit to the spectrometrically derived data reported here yields a value of 19 kcal/g-mole for both the CH and NH reactions. This difference may not be significant. Noise and measurement limitations when recording and analyzing the spectrometer output signals resulted in such imprecise data that a wide range of test temperatures would be required to yield accurate values of the activation energy. However, the temperature range of these tests was limited by the crystal phase change at 513°K and by film ignition at about 610°K, and thus it was not possible to obtain an accurate estimate of activation energy.

Although the fractional absorbance data in the total time range from 5 to 10 seconds does not appear to follow a first order kinetic law, a useful description of the reaction during this initial phase of the reaction can be obtained by a first order characterization fitted to the end points of this reaction period. Figure 27 shows this characterization as an Arrhenius plot for the rate constants of the CH and NH reactions. Table 3 summarizes these data. The least squares fit to these points yields activation energies of 19 kcal/g-mole for the NH reaction and 14 kcal/g-mole for the CH reaction, although a 30 kcal/g-mole activation energy would appear to be almost as reasonable an estimate for such scattered results. Also shown in Figure 27

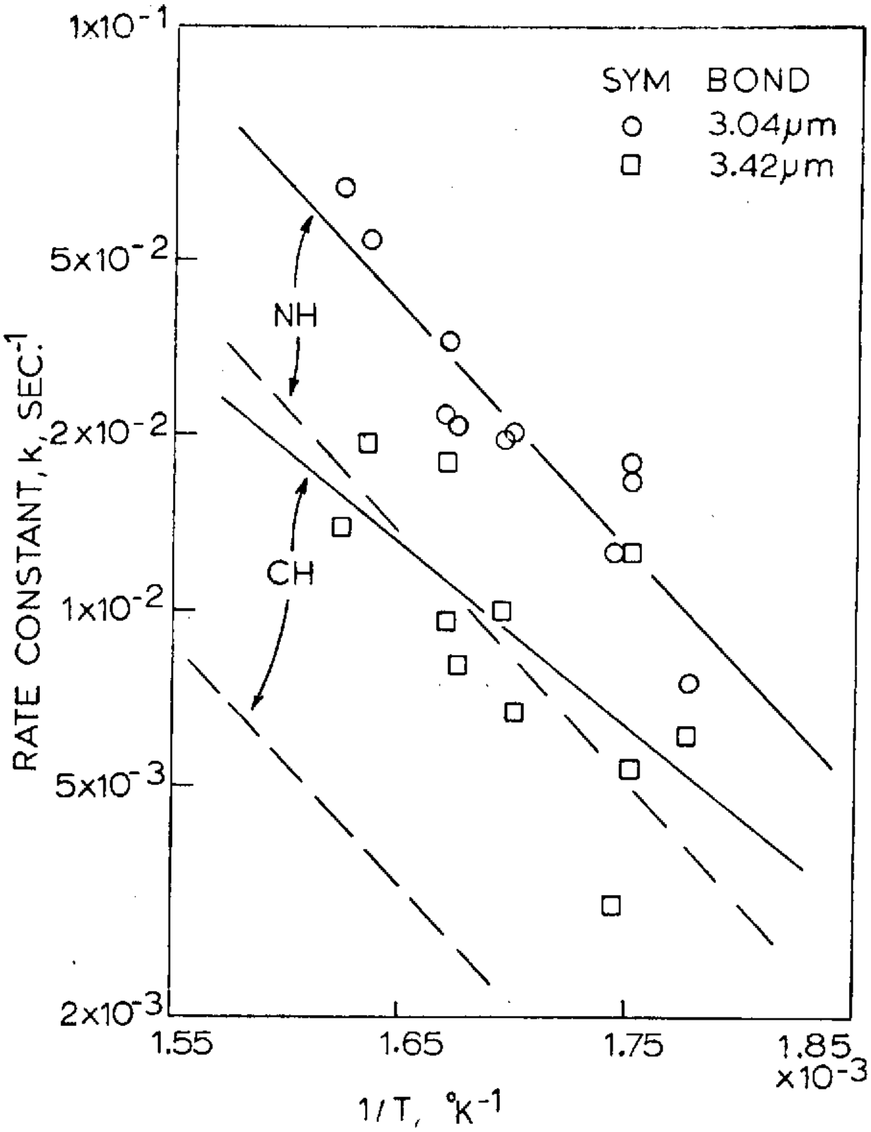

FIGURE 27. An Arrhenius plot is shown here for pseudo first-order rate constants from the fractional absorbance data obtained in the time interval of 5 to 10 seconds. These data are summarized in Table 3. The dashed lines are from Figure 26 for the rate constants obtained in the 10 to 60 second time period.

TABLE 3

A Summary of the NH and CH Pseudo First-Order Reaction Rate Constants for Total Times of 5 to 10 Seconds.

Temperature, °K	Reaction Rate Constant, sec^{-1}	
	NH Band	CH Band
594	2.31×10^{-2}	1.00×10^{-2}
597	2.06×10^{-2}	8.06×10^{-3}
571	1.77×10^{-2}	1.27×10^{-2}
560	7.45×10^{-3}	6.14×10^{-3}
573	1.23×10^{-2}	3.10×10^{-3}
571	1.66×10^{-2}	5.33×10^{-3}
587	2.01×10^{-2}	6.70×10^{-3}
590	1.96×10^{-2}	1.00×10^{-2}
598	2.89×10^{-2}	1.78×10^{-2}
615	5.30×10^{-2}	1.41×10^{-2}
611	4.27×10^{-2}	1.93×10^{-2}
598	2.08×10^{-2}	9.55×10^{-3}

are the least-squares lines for the NH and CH reactions from Figure 26 for the 10- to 60-second time interval. The average rate constants for the 5- to 10-second period are 2.5 and 4 times the values from the 10- to 60-second period. This result and the comparative data in Figure 26 illustrate what appears to be a correlation for the AP-polymer reaction. At a given temperature, the higher the heating rate employed or the shorter the time scale of observation, the higher the observed rate constants. Such an effect suggests the futility of trying to characterize these reactions for the very high heating rates encountered when burning a propellant at high pressures.

Summary and Conclusions

An in situ technique was developed and applied to the study of the ammonium-perchlorate-HTPB fuel-binder reaction. Thin films of the oxidizer loaded binder were heated at rates of 80 to 150°K/sec to preselected temperatures, and the infrared absorption spectra of the films were recorded at a rate of 8 persecond. The principal region scanned was from 2.5 to 5.5 μm, and the NH and CH absorption bands at 3.04 μm and 3.42 μm were monitored. Some tests were made in the 5.5- to 9.0-μm region to establish correspondence between the disappearance of the NH absorption at 3.04 μm and the ClO_2 absorption at 7.0 μm. A special high-intensity infrared radiation source was developed for this work.

Because of complexities in the aspectral absorption in the test films and the temperature dependence of the Beer-Lambert law absorption coefficient of the NH band, it was possible to obtain quantitative results only for tests at constant film temperatures and to measure only concentration changes. Tests were conducted at selected temperatures between the AP transition temperature of 513°K and the ignition temperature of about 610°K of the 30 percent AP films.

For times at temperature from 5 to 60 seconds, the NH and CH absorbance data were adequately described by a first order rate law. For a given temperature, the NH decomposition rate constant was essentially twice that of the CH, although because of the predominance of the polymer in the film, the total decomposition reaction was very fuel rich. The measured activation energy of both reactions was about 20 kcal/g-mole, and the reactions were coupled. The reaction rates were in order of mignitude agreement with values obtained from DSC and adiabatic heating tests.

For times at temperature less than 6 seconds, first-order rate constants were calculated from the initial and final value of the absorbances. For this time range, the rates were about three times the rates for the 5- to 60-second period. The estimated activation energy was also about 20 kcal/g-mole. For short times at temperature, the measured rate constants approached those derived from ignition tests. For the reactions studied here, the data suggest that the apparent reaction rates increase as the reaction time is shortened.

REFERENCES

1. Aiman, W. R., "Ammonium-Perchlorate Diffusion Flames - A Spectoscopic Investigation," Ph. D. Thesis, Department of Chemical Engineering, University of Utah, June 1968.

2. Aiman, W. R., Ryan, N. W. and Baer, A. D., "Ammonium-Perchlorate Diffusion Flames - A Spectroscopic Investigation," Technical Report under NASA Grant NGR-45-003-019, N68-36039 (1963).

3. Aiman, W. R., Baer, A. D., and Ryan, N. W., "The Chemical Arc: A Spectrometric Study," Western States Section/Combustion Institute, WSS/CI Paper 68-36, 1969 Spring Meeting, China Lake, Calif. April 1969.

4. Feinauer, L. R., "Characterization of Ignition from Flame Spectra of Radiatively Heated Propellant Samples," M. S. Thesis, Department of Chemical Engineering, University of Utah, June 1969.

5. Schulz, E. M., "Propellant-Flame Spectra During Depressurization," Ph. D. Thesis, Department of Chemical Engineering, University of Utah, June 1970.

6. Schulz, E. M., Baer, A. D., and Ryan. N.W., "Technical Report of Emission Spectra and Temperature of Composite Propellant Flames During Depressurization," under NASA Grant NGL-45-003-017, Department of Chemical Engineering, University of Utah (May, 1973).

7. Ryan, N. W., Schulz, E. M., and Baer, A. D., "Emission Spectra from Propellant Flames During Depressurization,' Third ICRPG/AIAA Solid Propulsion Conference, CPIA Pub. No. 167, June 1968.

8. Bear, A. D., Ryan, N. W., and Schulz, E. M. "Spectra and Temperature of Propellant Flames During Depressurization," *AIAA Journal, 9* 869 (1971).

9. Gross, R. M., "Absorption Spectra of High-Temperature Solid Propellant Flames," Technical Report under Grant AFOSR 73-2470A, Department of Chemical Engineering, University of Utah, August 1974.

10. Eisel, J. L., "Flame Spectra of Solid Propellants During Unstable Combustion," Ph. D. Thesis, Department of Chemical Engineering, University of Utah, June 1972.

11. Eisel, J. L., Ryan, N. W., and Baer, A. D., "Spectral and Temporal Resolution of Propellant Flames during Bulk-Mode Instability," *Eighth JANNAF Combustion Meeting, I* (CPIA Pub. No. 220; 1971) 373-386.

12. Eisel, J. L., Ryan, N. W., and Baer, A. D. "Combustion of NA_4ClO_4- Polyurethane Propellants: Pressure, Temperature, and Gas Phase Compositional Fluctuations," *AIAA Journal, 10*, 1655 (1972).

13. Mal'tsev, V. and Summerfield, M. "Investigation of the Spectral Radiation Characteristics of the Flame-jet of Nitrate-Ester Propellants Containing Platonizing Catalysts," Submitted for publication to *Combustion and Flame*.

14. Bouck, L. S., Baer, A. D., and Ryan, N. W. "Pyrolysis and Oxidation of Polymers at High Heating Rates," *Twelfth Symposium (International) on Combustion*. Pittsburgh, Pennsylvania: The Combustion Institute, 1139 (1973).

15. Cheng, J. T., Ryan, N. W., and Baer, A. D. "Oxidative Decomposition of PBAA Polymer at High Heating Rates," *Twelfth Symposium (International) on Combustion*. Pittsburgh, Pennsylvania: The Combustion Institute, 525 (1969).

16. Inami, S. H., Rosser, W. A., Jr., and Wise, J., "Heat-Release Kinetics of Ammonium Perchlorate in the Presence of Catalysis and Fuel," *Combustion and Flame, 12,* 41 (1968).

17. Simon, D. R., "Rapid Linear Pyrolysis of Composite Solid Ingredients," Report NASA CR-66856 under Contract No. NAS1-8450, Vitro Laboratories, Silver Springs, Md., September 1970.

18. Boggs, T. L., "Deflagration Rate, Surface Structure and Subsurface Profile of Self-Deflagrating Single Crystals of Ammonium Perchlorate," *AIAA Journal, 8,* 867 (1970).

19. Schmidt, W. G., "The Effect of Solid Phase Reactions on the Ballistic Properties of Propellants," Report No. NASA CR 112083, (N72-21809) under Contract NAS1-9463, Aerojet Solid Propulsion Co. Sacramento, Calif., August 1972.

20. Baer, A. D., and Ryan, N. W. "Evaluation of Thermal-ignition Models from Hot-wire Ignition Tests," *Combustion and Flame, 15*, 9 (1970).

21. Dauerman, L., "Solid State Reactions in Solid Propellants," Report under Contract AFOSR-1491-68, Department of Chemical Engineering, New York University, University Heights, New York, N. Y. March 1970.

22. Hartman, K. O., and Musso, R. C., "The Thermal Decomposition of Nitroglycerine and Its Relationship to the Stability of CMDB Propellants," Paper 72-30, Fall Meeting of the West Coast Section, The Combustion Institute, Monterey, Calif., October 1972.

23. Carslaw, H. S. and Jaeger, J. C., *Conduction of Heat in Solids, 2nd Ed.:* London: Oxford University Press (1959).

24. Law, R. J., "Reactions in Solid Propellants from Infrared Spectra," Ph. D. Thesis, Department of Chemical Engineering, University of Utah (1975).

25. Mihlfeith, C. M., Baer, A. D., and Ryan, N. W. "The Response of a Burning Solid Propellant Surface to Thermal Radiation." AFOSR Scientific Report No. TR-71-2664, AD-736049 (1971).

26. Law, R. J., Baer, A. D., and Ryan, N. W., "A Spectrometric Study of Pyrolysis Reactions of Polyurethane," *West Coast Section, The Combustion Institute,* Paper 73-11 (1973).

27. Jacobs, P. W. M., and Russell-Jones, A., "The Decomposition and Ignition of Mixtures of Ammonium Perchlorate and Copper Chromate," *Eleventh Symposium (International) on Combustion,* Pittsburgh, Pennsylvania: The Combustion Institute, 457 (1967).

28. Waesche, R. H. W., "Research Investigation of the Decomposition of Composite Solid Propellants, " United Aircraft Research Laboratories Report G910476 - 24 on Contract NAS7-481 (1969).